Seminar, Fudan University, Nov 21, 2024

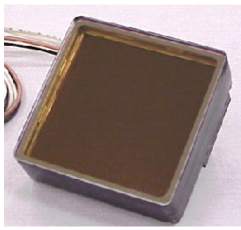

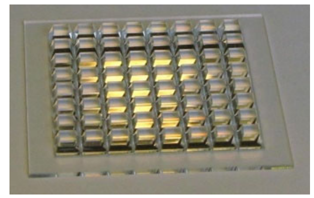
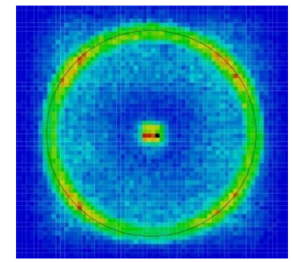
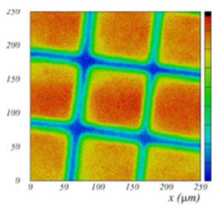
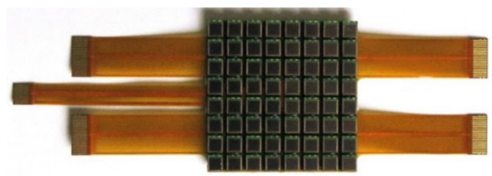


Novel photon detectors

Peter Križan

University of Ljubljana and J. Stefan Institute

Introduction: why?

Photon detectors are at the heart of most experiments in particle physics.

Subsystems with photosensors in the Belle II Detector

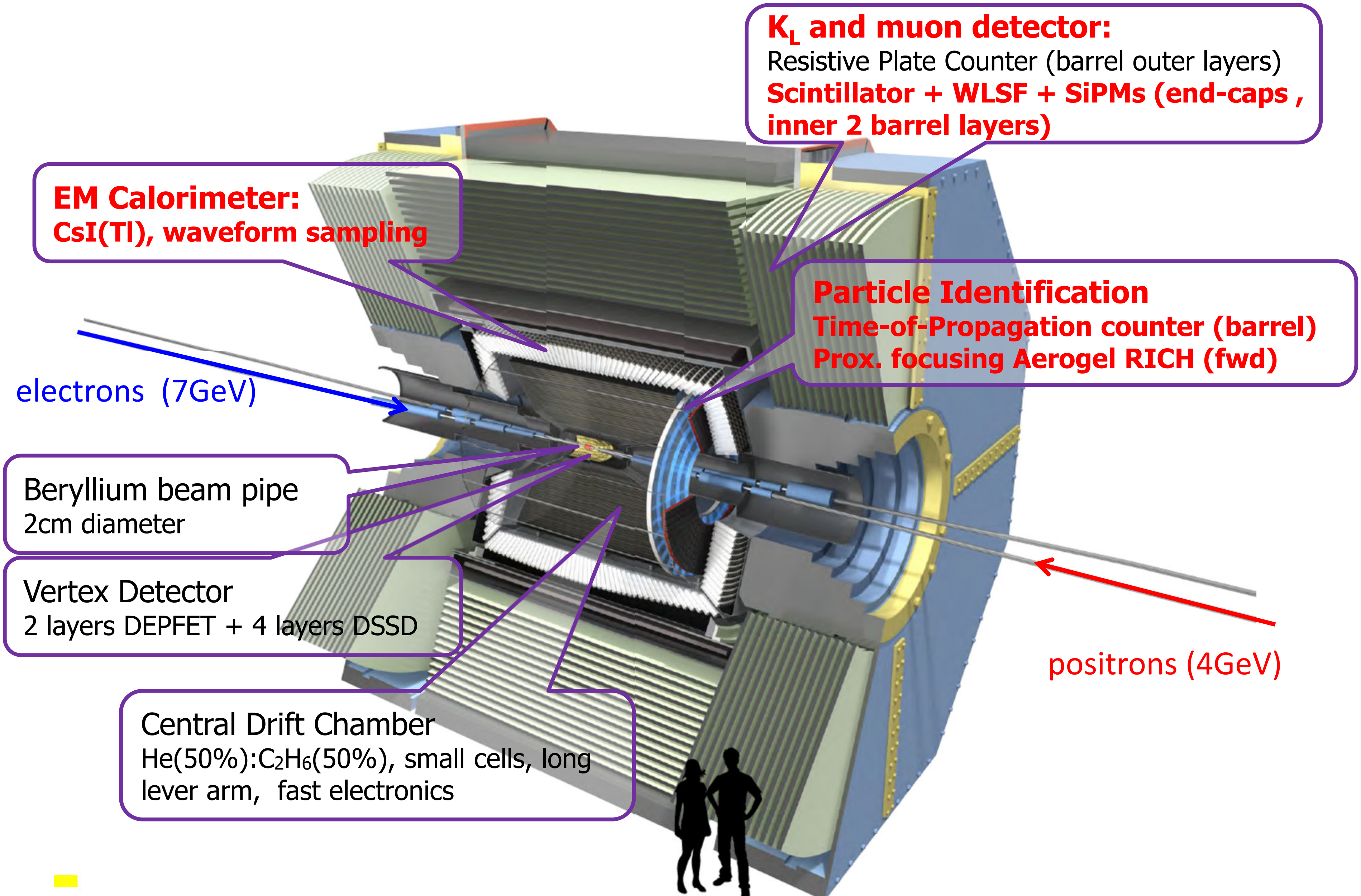

Subsystems with photosensors in LHCb

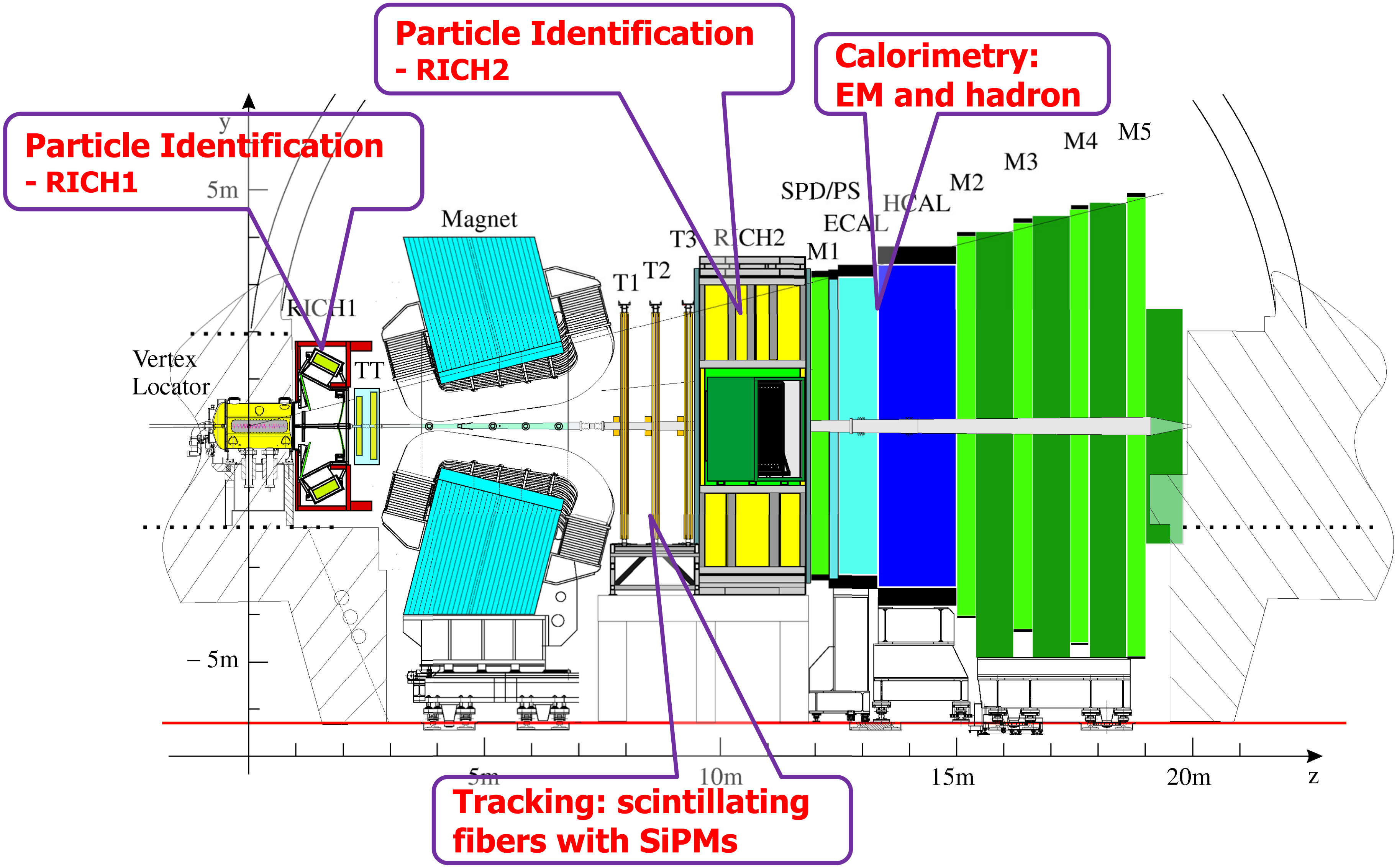

Components with photosensors in CMS

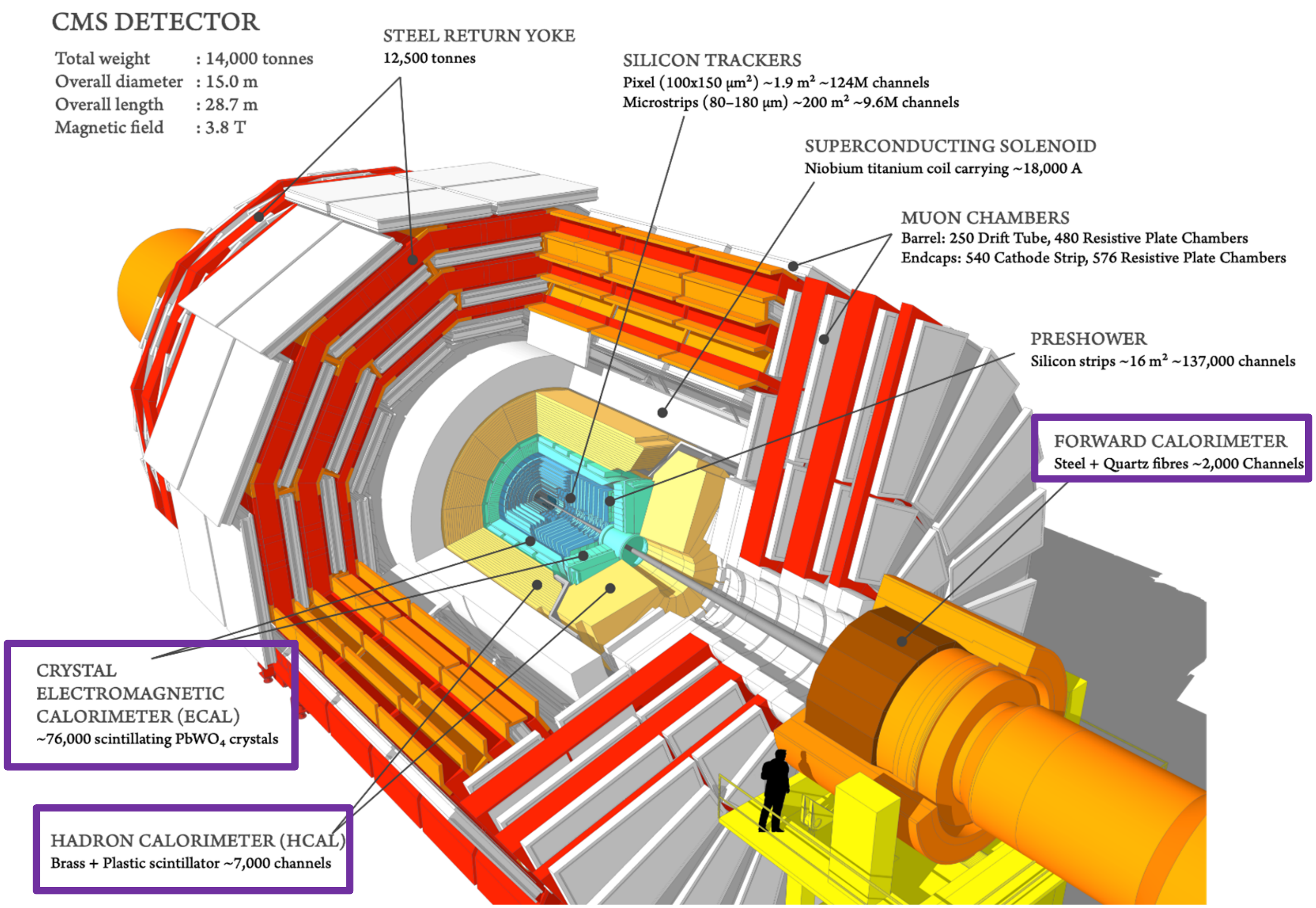

Photosensors in neutrino experiments: JUNO

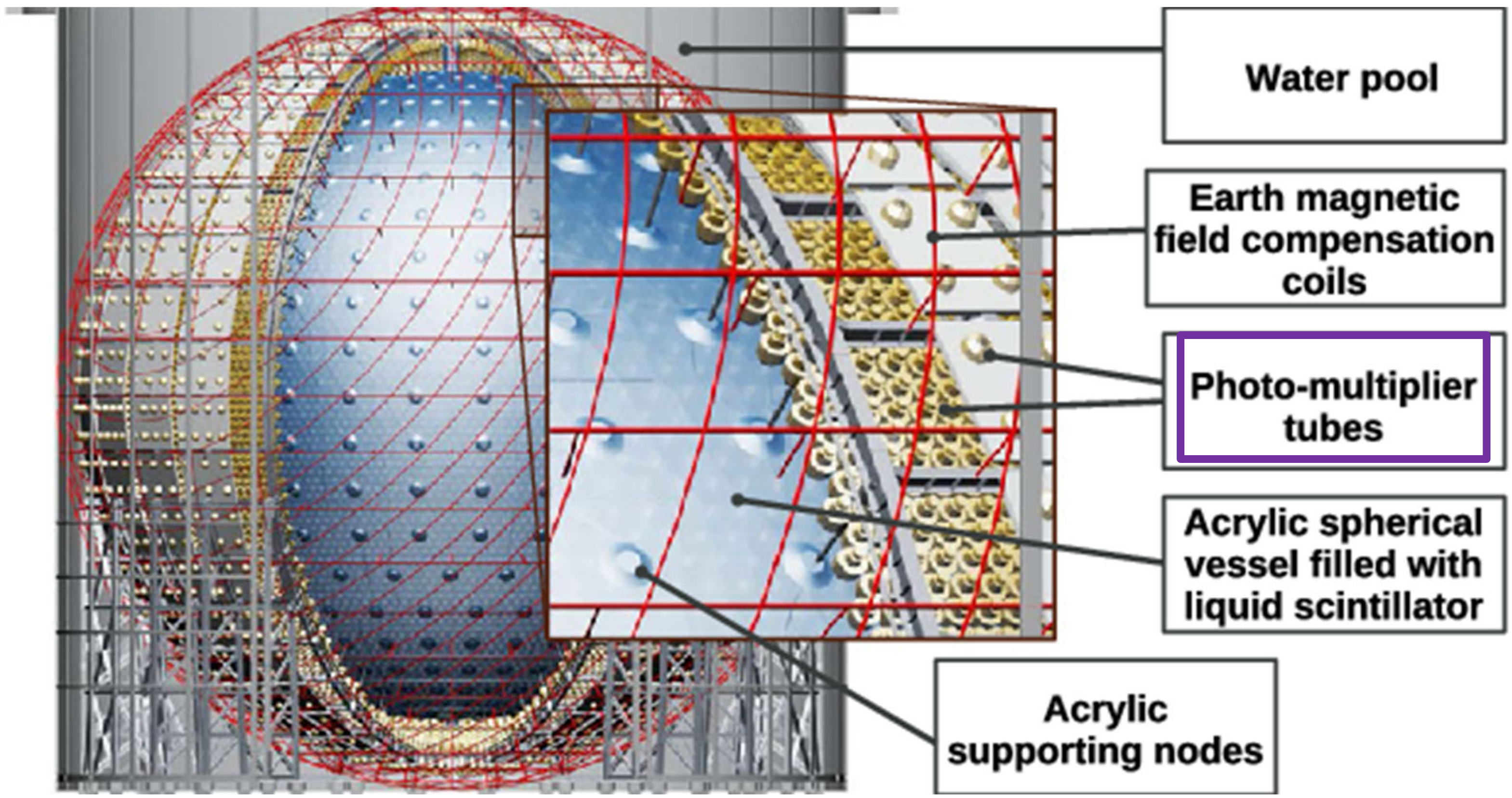

… a paramount component

Photosensors in dark matter experiments

Example: XENON1T

- 1 tonne of liquid Xenon + a gas layer
- Gran Sasso Laboratory LNGS

- S1: scintillations in liquid Xenon (small signal, top and bottom)
- S2: scintillations in the gas phase where electrons get accelerated (large signal, top only)
- Time difference: depth of interaction point

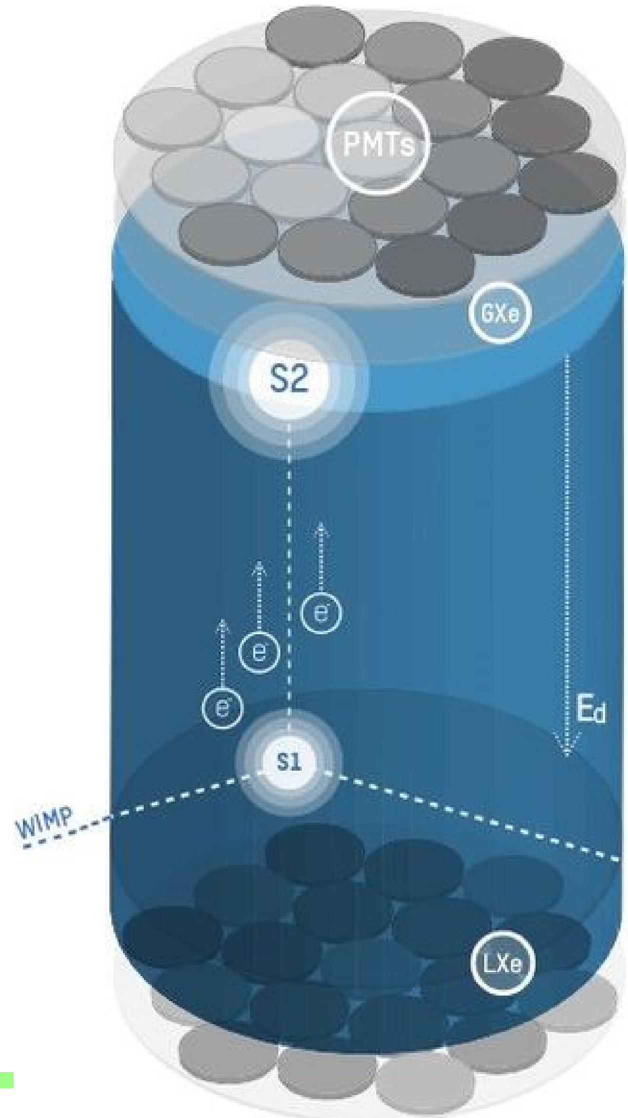

Introduction: why?

Photon detectors are at the heart of most experiments in particle physics.

Moreover, they are also finding application in other scientific fields (chemistry and biology) and are ubiquitous in society in general.

New environments where we need to detect light (in particular low light levels) → need advances in existing technology and transformative, novel ideas to meet the demanding requirements.

Two main lines of R&D are pursued at present:

- Enhance timing resolution.
- Develop photosensors for extreme environments.

Belle II detector: subsystems with R&D for potential photosensor upgrades

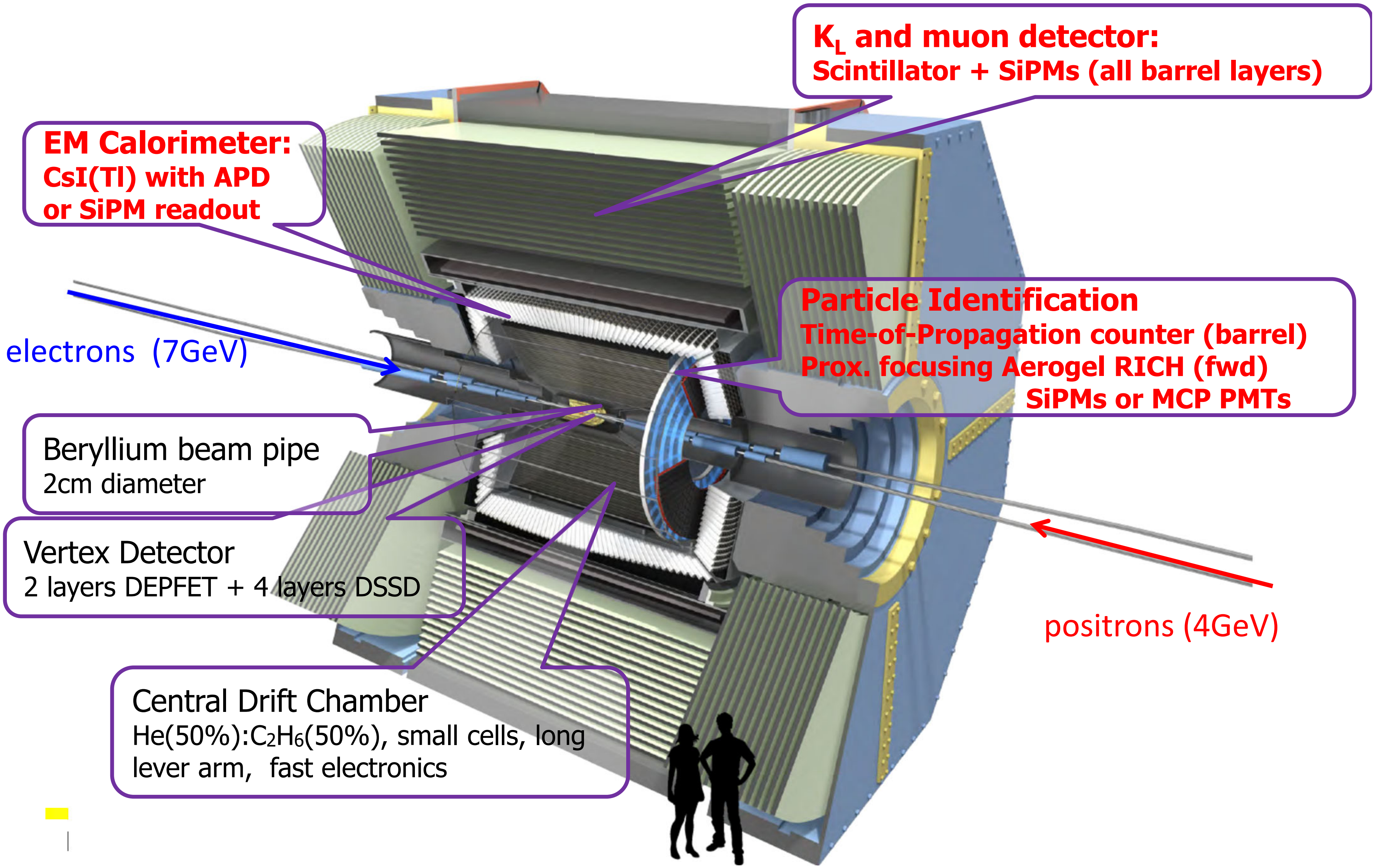

Contents

Introduction: why and what kind of photosensor?

Vacuum-based photodetectors

Solid state low light level photosensors

Photodetector R&D at Belle II

Summary and outlook

Vacuum-based photodetectors

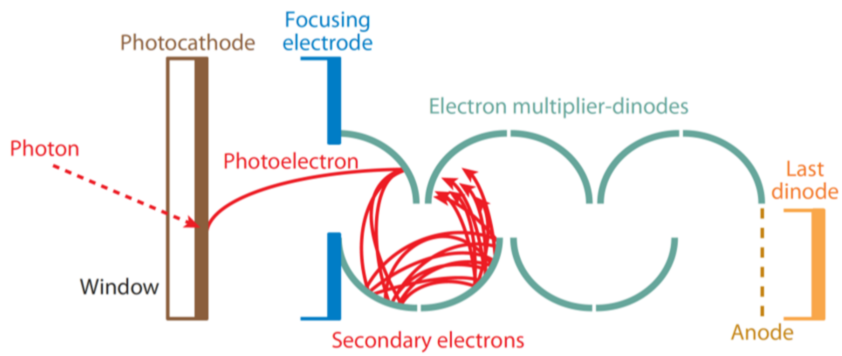

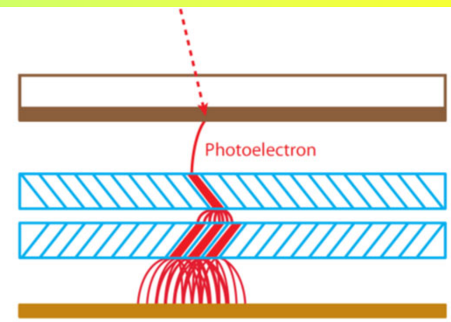

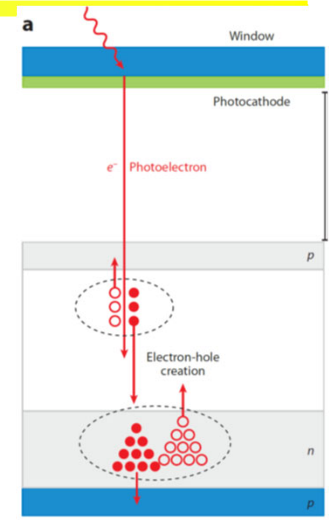

Generic steps:

- Photon → photo-electron conversion in the photocathode
- Photo-electron collection in the multiplication system
- Mutiplication (dynodes, microchannel plates, high E field + Si)
- Signal collection

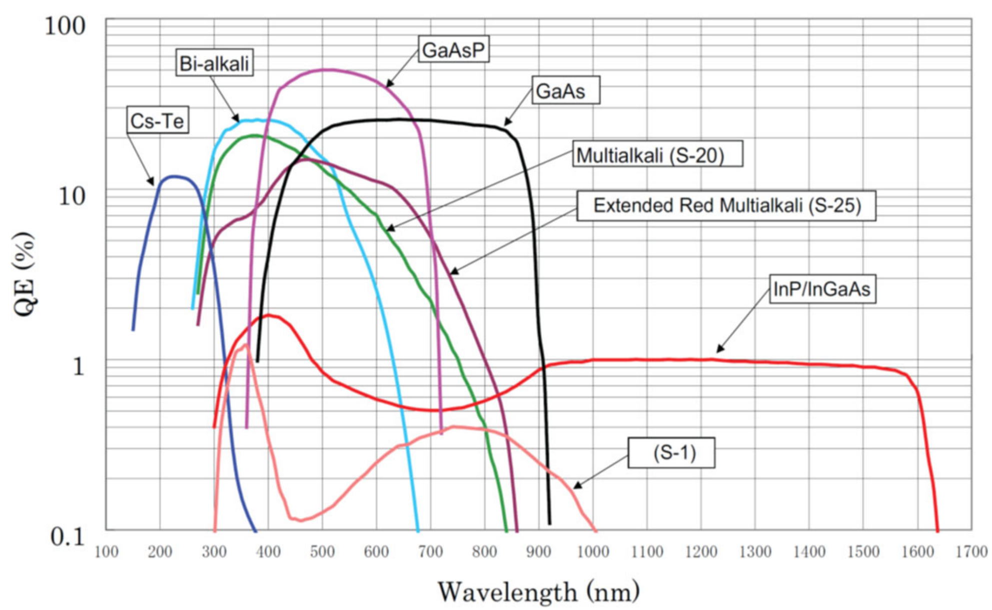

Photomultiplier tube (PMT)

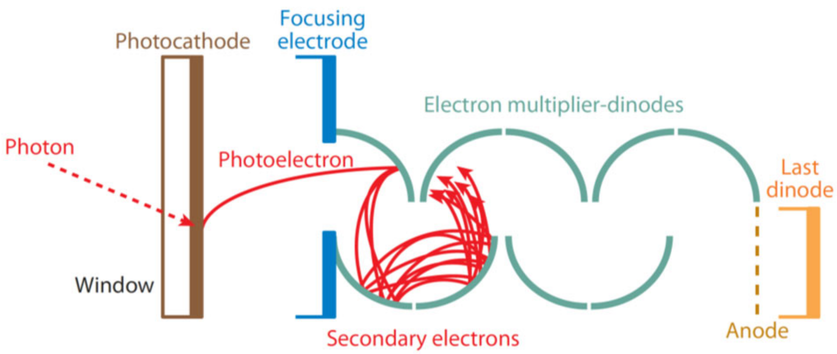

Multiplication on an array of electrodes coated by a secondary emitter material: 1 incoming electron → ~3-4 emitted electrons

Masatoshi Koshiba, Nobel prize 2002 (together with R. Davis)

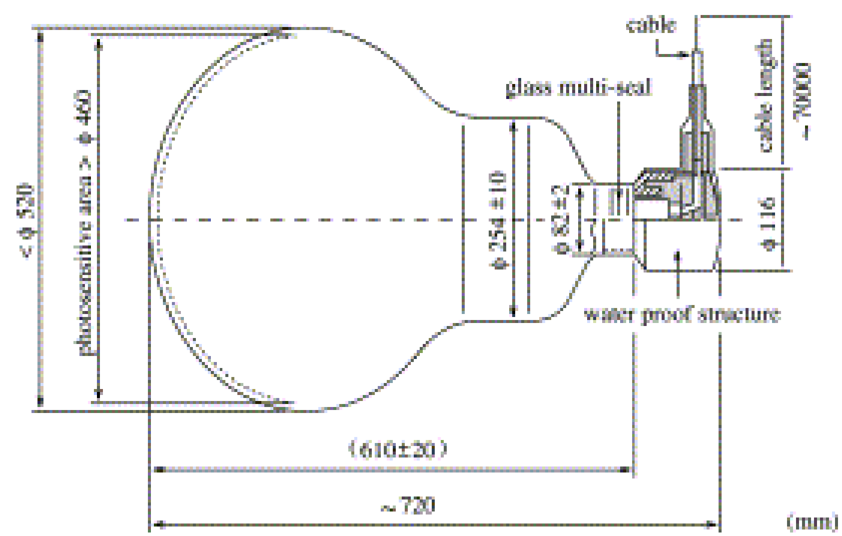

Multianode photomultiplier tube (MA-PMT)

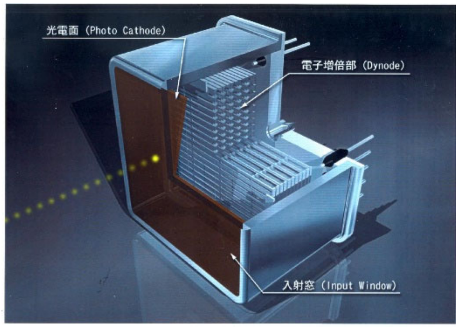

Hamamatsu R5900 (and follow ups 7600, 8500)

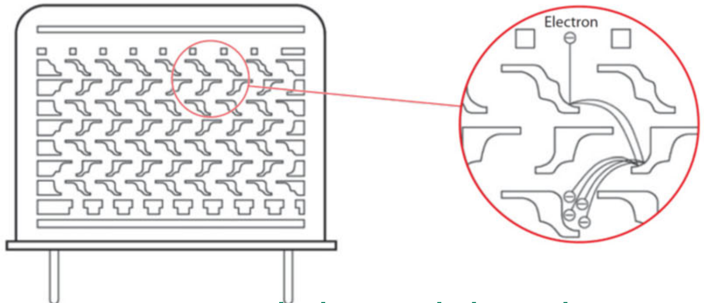

Metal channel dynodes

Response to single photons

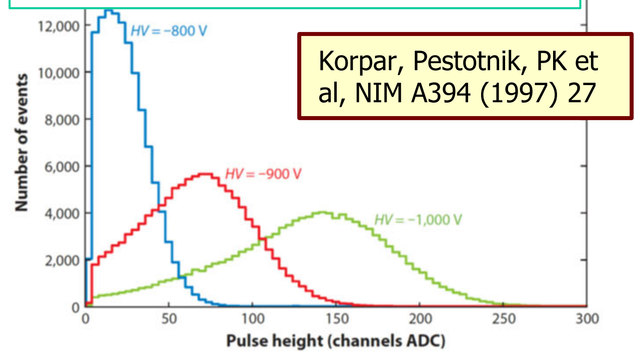

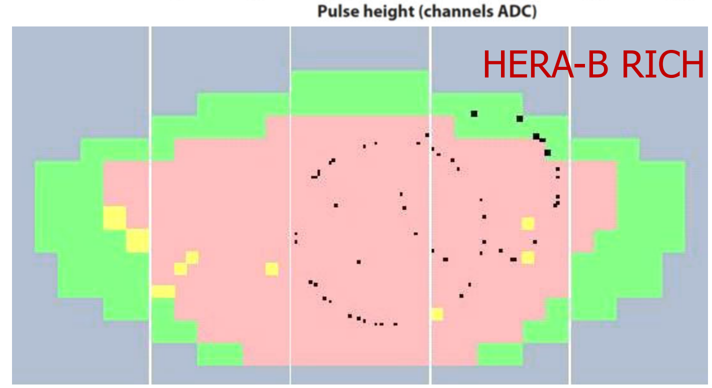

Pioneered in the HERA-B RICH, later used in the COMPASS, CLASS12 and GlueX RICH detectors

Recent use in the upgraded LHCb RICH detectors; planned for CBM RICH

Excellent performace (excellent single photon detection efficiency, very low noise, low cross-talk), best choice for large areas with no B field

Micro Channel Plate PMT (MCP-PMT)

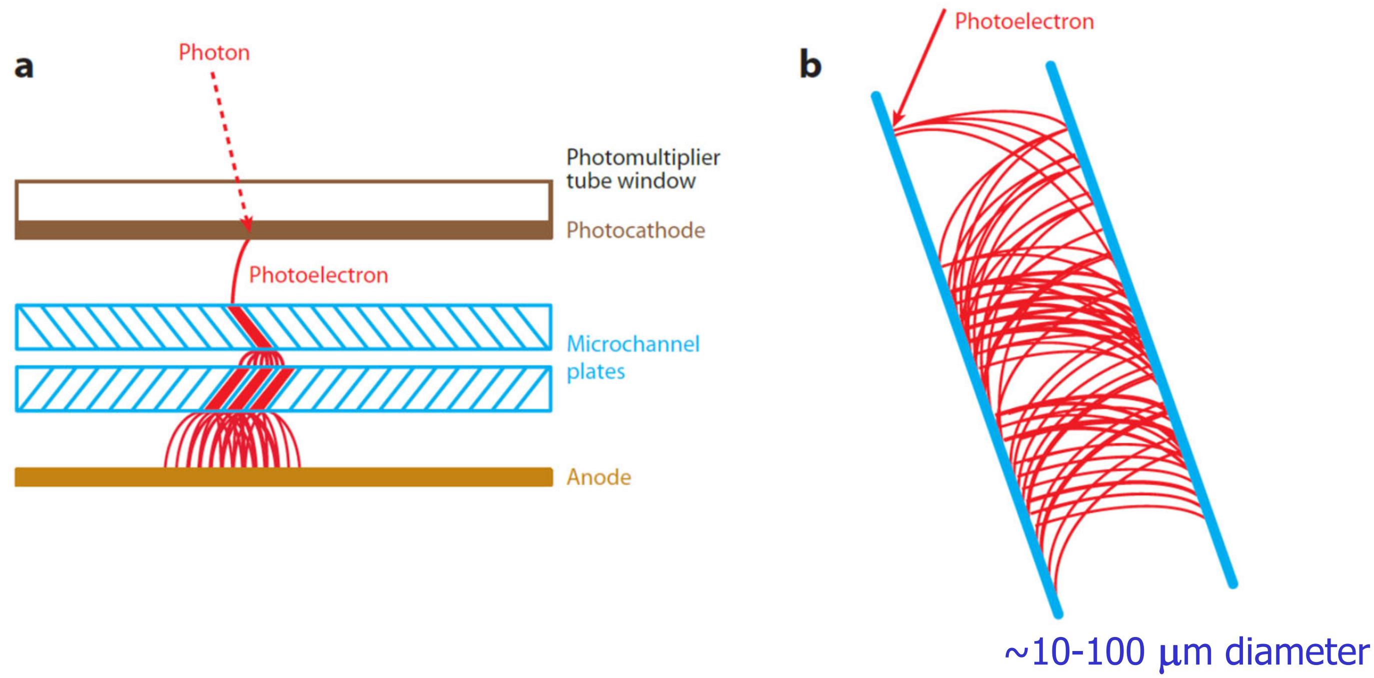

Multiplication step: a continuous dynode – a micro-channel coated with a secondary emitter material

Micro Channel Plate PMT (MCP-PMT)

Similar to ordinary PMT – the dynode structure is replaced by MCPs.

Basic characteristics:

- Gain ~ 10^6 → single photon
- Collection efficiency ~ 60%
- Small thickness, high field → small TTS
- Works in magnetic field
- Segmented anode
  → position sensitive

MCP is a thin glass plate with an array of holes (<10-100 μm diameter) - - a continuous dynode structure

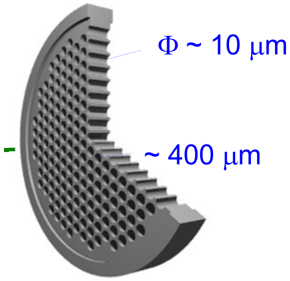

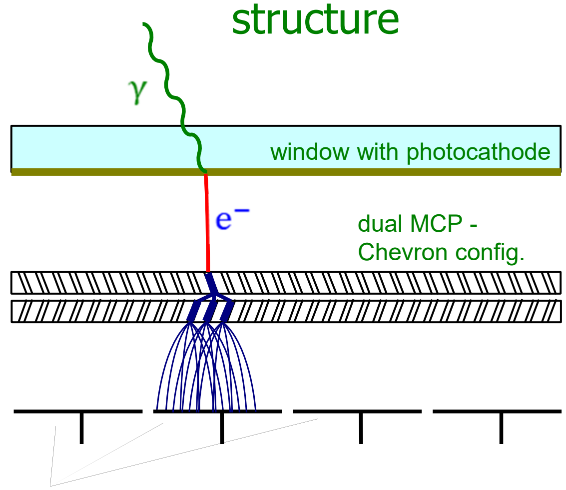

Anodes → can be segmented according to application needs

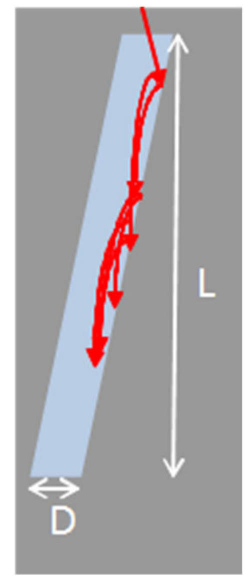

MCP gain depends on L/D ratio – typically 1000 for L/D=40

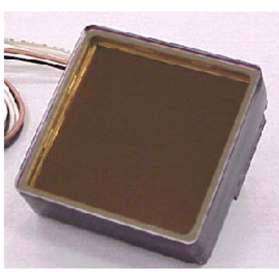

PHOTONIS

2″

1″

HAMAMATSU

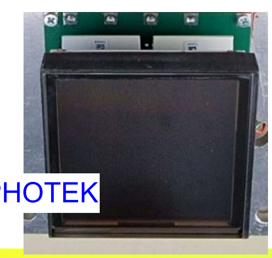

PHOTEK

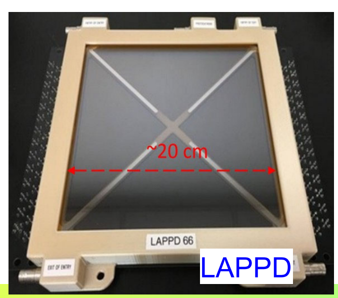

LAPPD

8″

Micro Channel Plate PMT: properties

Very fast: single photon detection with sigma of ~30-40 ps

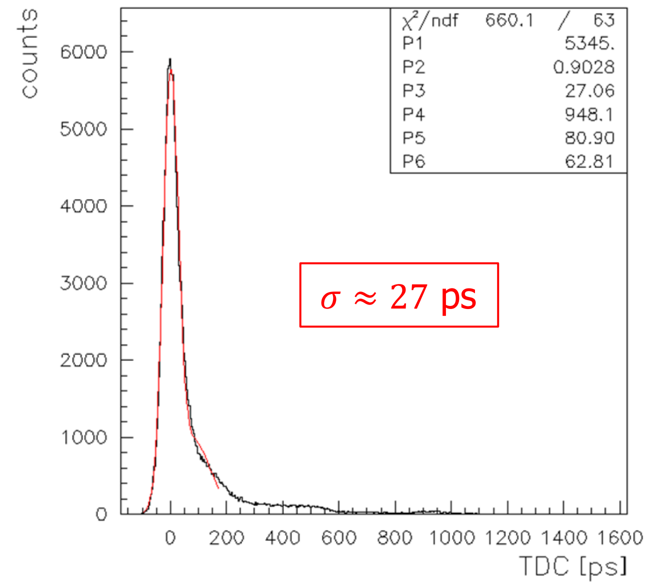

MCP PMTs work well in magnetic fields

→ performance depends on the diameter of the micro-channels

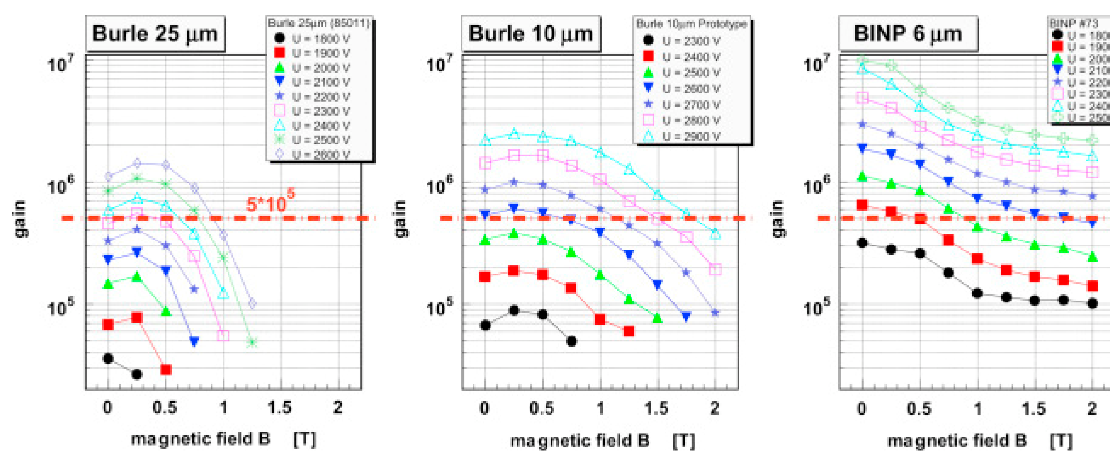

MCP-PMT: single photon pulse height and timing

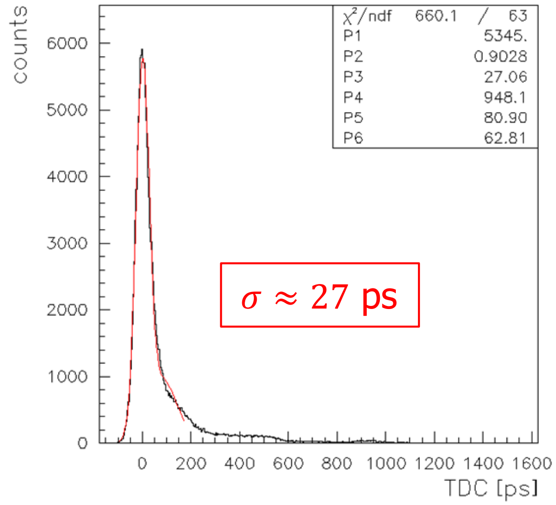

Photoelectron back-scattering produces a rather long tail in timing distribution and position resolution.

Photoelectron backscattering reduces collection efficiency and gain, and contributes to cross-talk in multi-anode PMTs

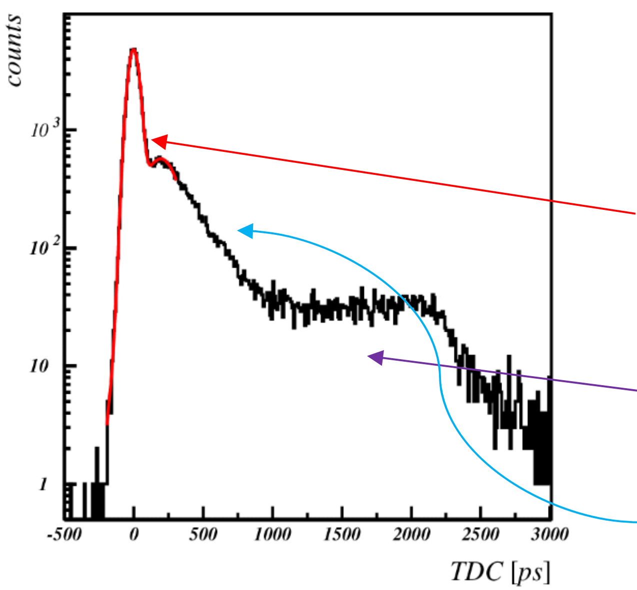

Typical single photon timing distribution with a narrow main peak (σ~30-40 ps) and contributions from photoelectron elastic back-scattering (flat distribution) and inelastic back-scattering.

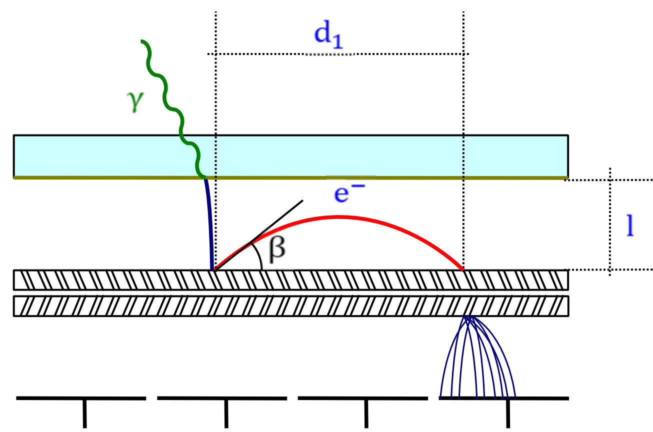

S.Korpar@PD07

Modelling MCP-PMT: Photoelectrons in a uniform electric field

Photoelectrons travel from the photocathode to the electron multiplier (uniform electric field $\frac{U}{l}$, initial energy $E_0 \ll Ue_0$):

- photoelectron range

$$d_0 \approx 2l\sqrt{\frac{E_0}{Ue_0}}sin(\alpha)$$

- and maximal travel time (sideway start)

$$t_0 \approx l\sqrt{\frac{2m_e}{Ue_0}}$$

- time difference between downward and sideways initial direction

$$\Delta t \approx t_0\sqrt{\frac{E_0}{Ue_0}}$$

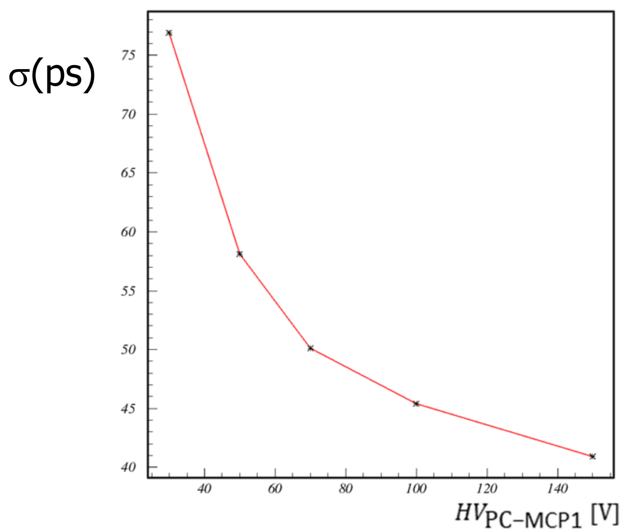

Time resolution vs PC-MCP1 voltage

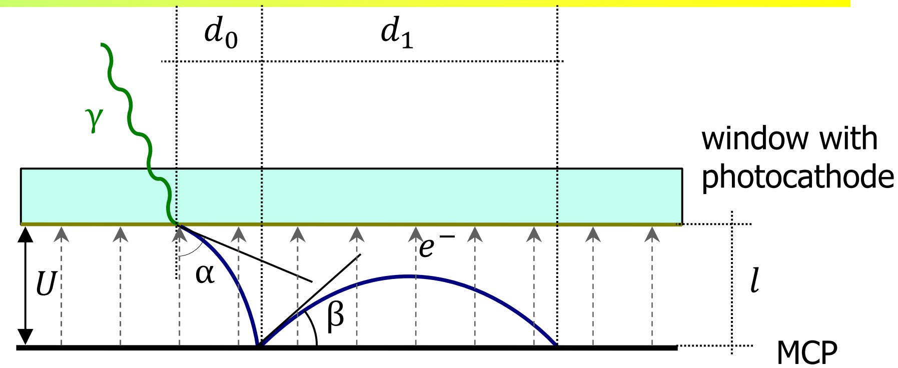

Backscattering delay and range (maximum for elastic scattering):

- maximum range vs. angle

$$d_1 = 2lsin(2\beta)$$

  maximum range for backscattered photoelectron is twice the photocathode – first electrode distance
- maximum delay vs. angle

$$t_1 = 2t_0sin(\beta)$$

  maximum delay is twice the photoelectron travel time
- time of arrival of elestically scattered photoelectrons: flat distribution up to max $t_1 = 2t_0$

Example ($U = 200$ V, $E_0 = 1$eV, $l = 6$mm)

photoelectron:
- max range $d_0 \approx 0.8$ mm
- p.e. transit time $t_0 \approx 1.4$ ns
- $\Delta t \approx 100$ ps

backscattering:
- max range $d_1 = 2l = 12$ mm
- max delay $t_1 = 2.8$ ns

S.Korpar@PD07

Modelling MCP-PMT: time resolution vs photocathode-to-microchannel-plate voltage difference

Time difference between downward and sideways initial direction (previous slide)

$$\Delta t \approx t_0 \sqrt{\frac{E_0}{U e_0}}$$

This difference is proportional to the time resolution – sigma of the main peak in the time response of the MCP-PMT

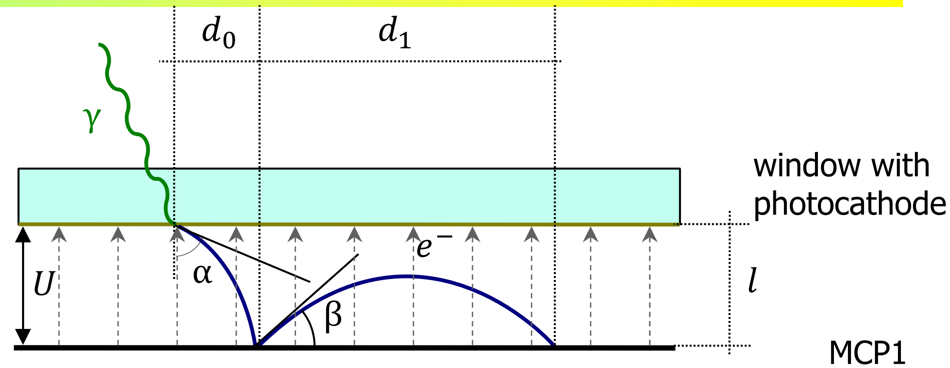

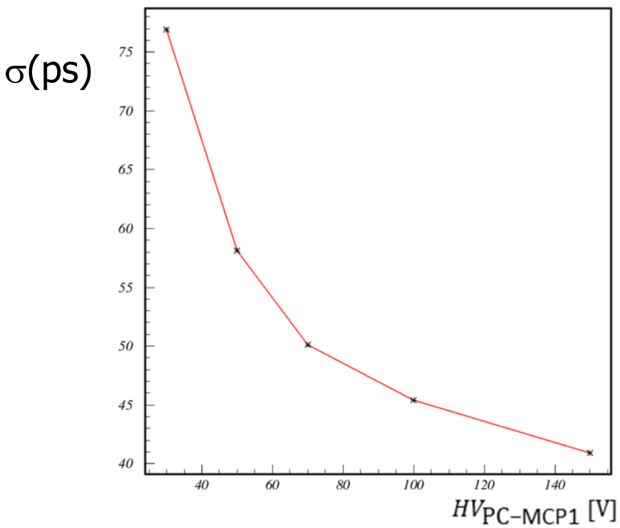

Time resolution vs PC-MCP1 voltage U

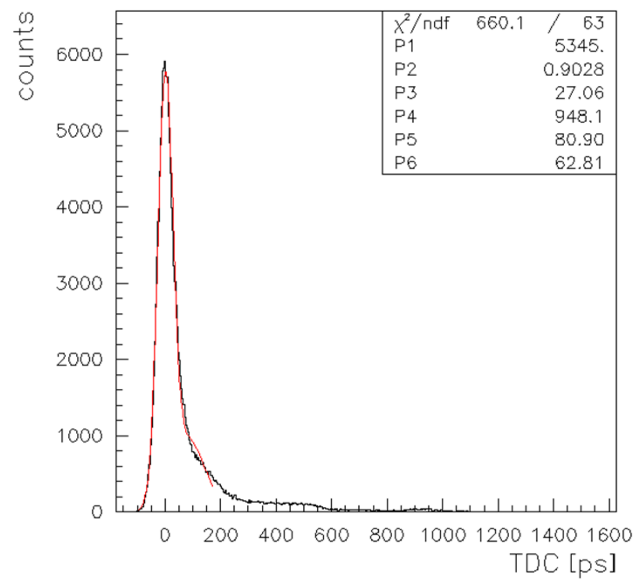

S. Korpar et al., to be submitted to NIMA

LAPPD (large area picosecond photodetector) Gen II

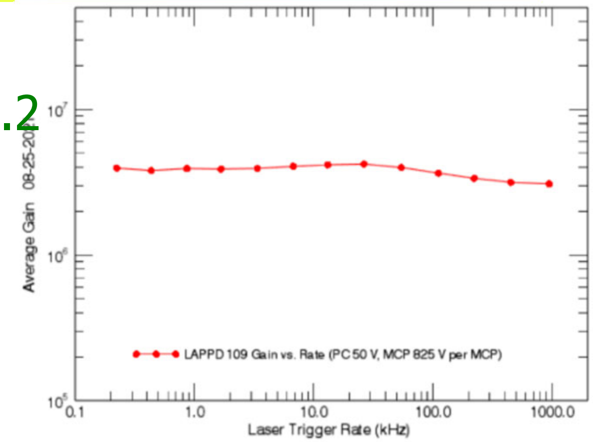

Characteristics (Incom):

- size 230 mm x 220 mm x 22 mm (243 mm x 274 mm x 25.2 mm with mounting case)
- borosilicate back plate with interior resistive ground plane anode – 5 mm thick
- capacitively coupled readout electrode
- MCPs with 20 μm pores at 20 μm pitch
- two parallel spacers (active fraction ≈ 97 %)
- gain $\approx 5 \cdot 10^6$ @ ROP (825 V/MCP, 100 V on photocathode)
- peak QE $\approx 25\%$
- Dark Count rate @ ROP: ~ 70 kHz/cm2 with 8×10^5 gain

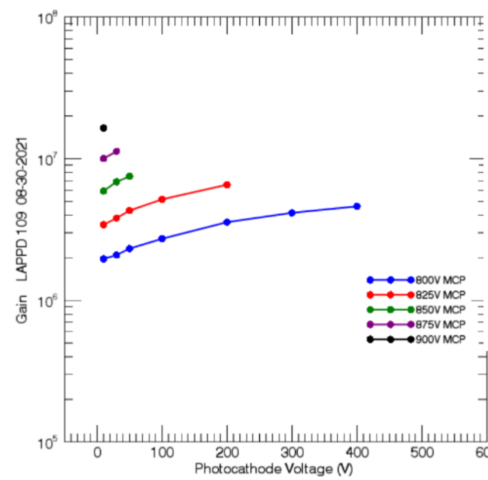

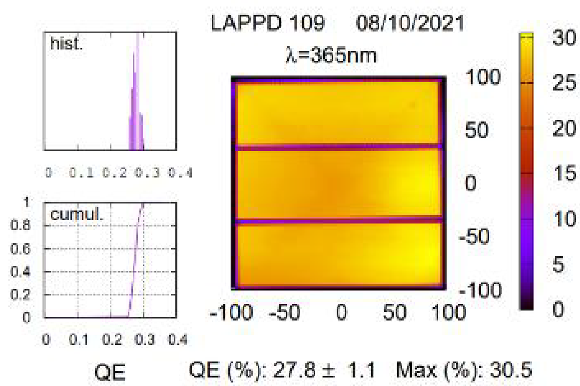

MCP PMT ageing

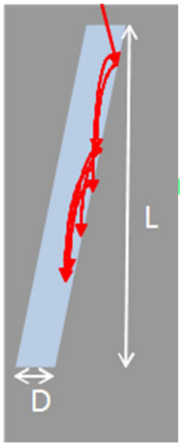

MCP PMTs: photo-cathode degradation due to ion feedback, main concern in high intensity experiments.

Ions are liberated from the microchannel walls during the multiplication process.

→ Long-standing problem for this sensor type.

K. Inami, 2021, Talk at ECFA TF4 Symposium

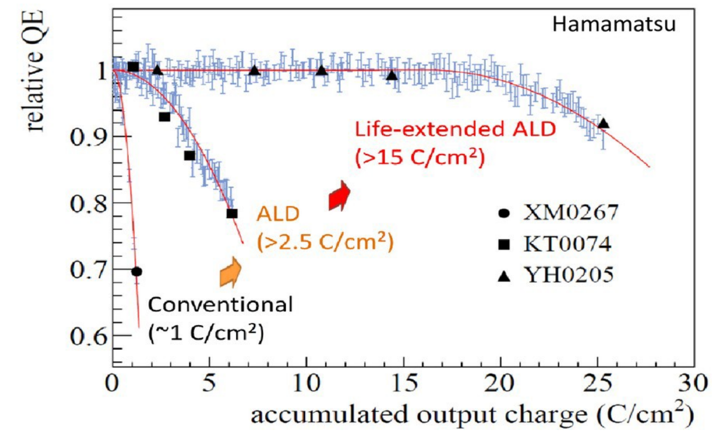

ALD (atomic layer deposition) coating of MCP microchannels → ~100x photo-cathode lifetime increase

- Hamamatsu 1-inch YH0205 (>20 C/cm²) [K. Inami, 2021]
- No QE degradation for Photonis MCP-PMT (R2D2) to >34 C/cm²
- Little QE degradation in LAPPD 8-inch up to 5.6 C/cm² [V. A. Chirayath, CPAD2021]

A. Lehmann, RICH2022

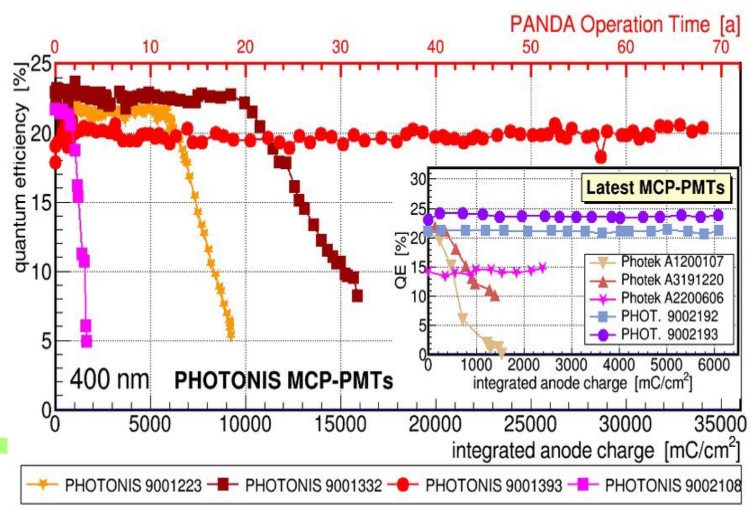

V.A. Chirayath et al., Talk at CPAD 2021

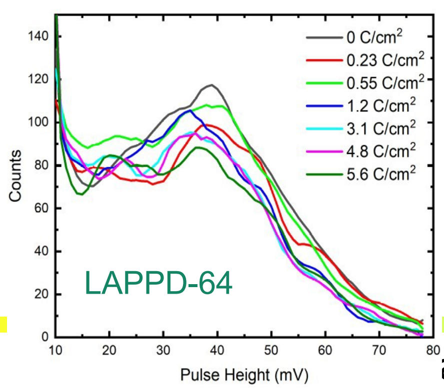

Possible Future of Electron Multiplication

Tynodes (→ Time Photon Counter)

- Transmission mode dynode → tynode
- Fabrication of tynodes (MgO ALD, diamond) using MEMS technology
- “Anode” is a CMOS chip (e.g., TimePix)
- Very promising properties
  - Very compact; high B-field tolerance; very fast
  - Very low DCR; very good 2D spatial resolution

H. van der Graaf et al., NIM A847 (2017) 148

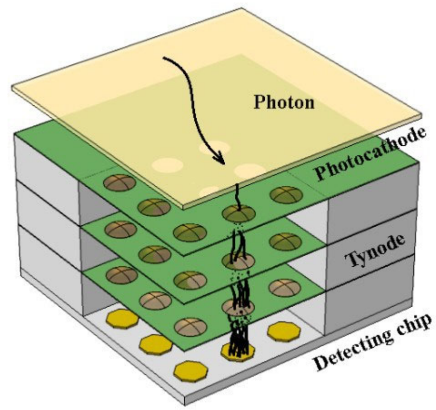

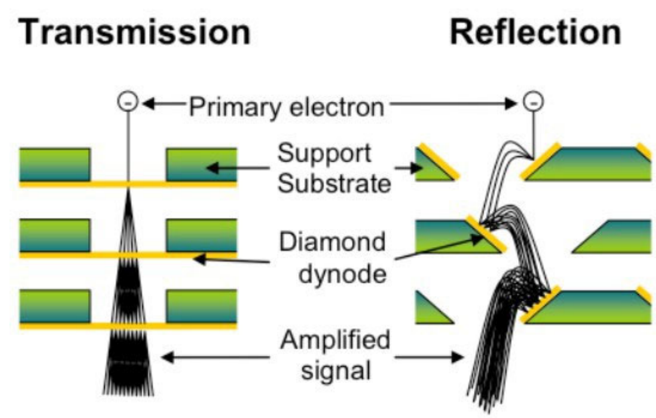

MCP-PMT with CMOS anode

Conceptual design for 4D detection of single photons

- Hybrid concept: MCP-PMT where the pixelated anode is an ASIC (CMOS) embedded inside the vacuum
- Prototype with Timepix4 ASIC as anode (array of 23k pixels)

Envisaged performance

- <100 ps time resolution and 5-10 μm spatial resolution
- Rate capability of >100 MHz/cm² (<2.5 Ghits/s @ 7 cm² area)
- Low gain (~10^4) operation possible → x100 lifetime increase

M. Fiorini, RICH2022

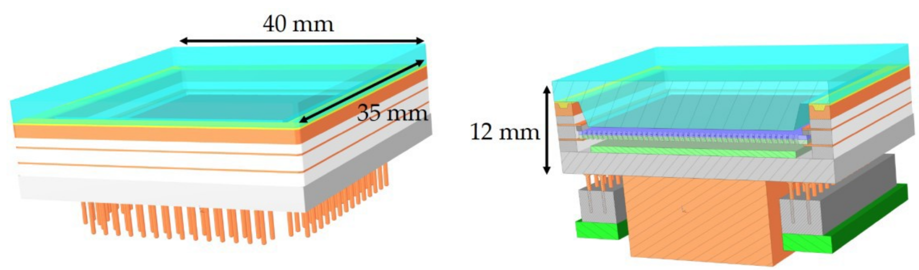

Hybrid photodetectors (HPD, HAPD)

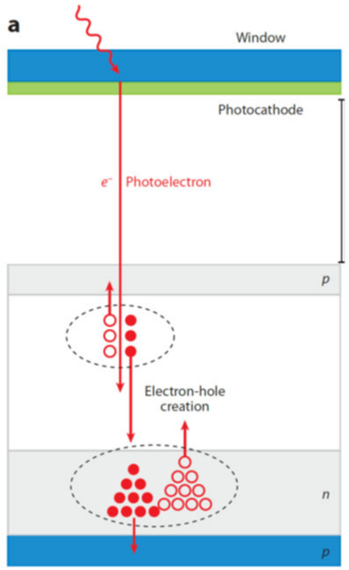

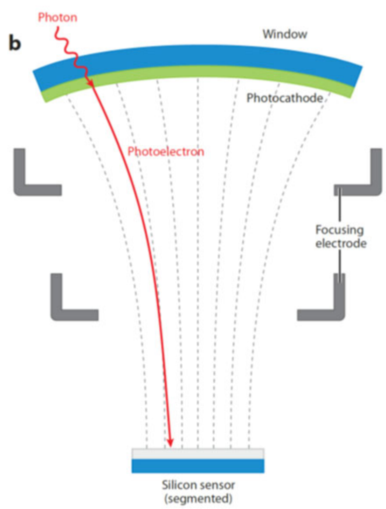

Focusing and proximity focusing configurations

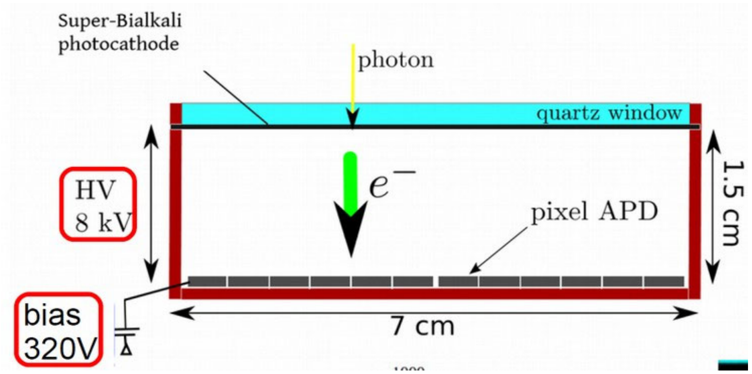

Photo-electron acceleration in a static electric field (8kV to 25 kV)

Photo-electron detection with

- Segmented PIN diode (HPD)
- Avalanche photo diode (HAPD)
- Silicon photomultiplier (VSiPMT)

Employed on a large scale:

- HPD: RICH1+RICH2 of LHCb (Run 1+2), CMS HCAL
- HAPD: Aerogel RICH detector of Belle II

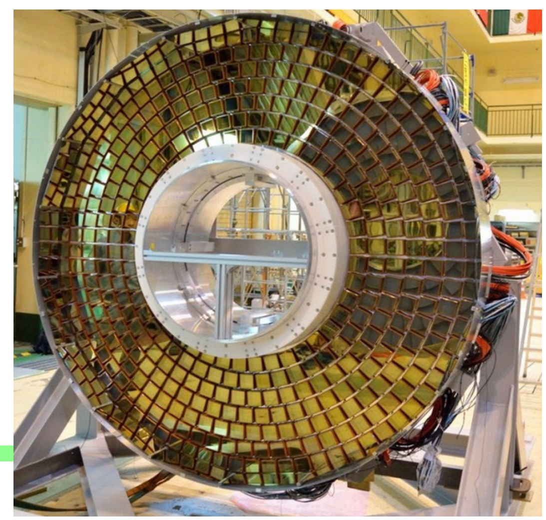

HAPD: photoelectron backscattering in magnetic field

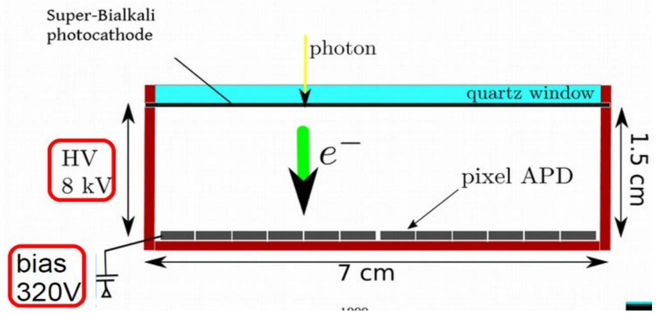

In the HAPD of the Belle II ARICH, around 20% of photoelectrons back-scatter and the maximum range is twice the distance from photocathode to APD ~40mm (similar to MCP-PMT).

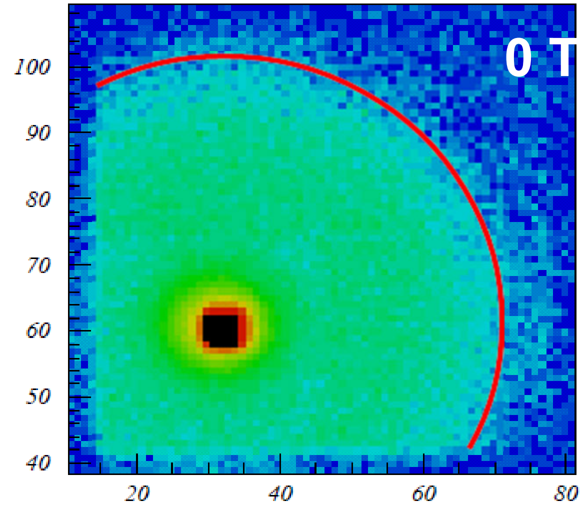

In magnetic field (perp. to the HAPD window) scattered photoelectrons follow magnetic field lines and fall back to the same pad

Photoelectron energy is deposited at the same pad

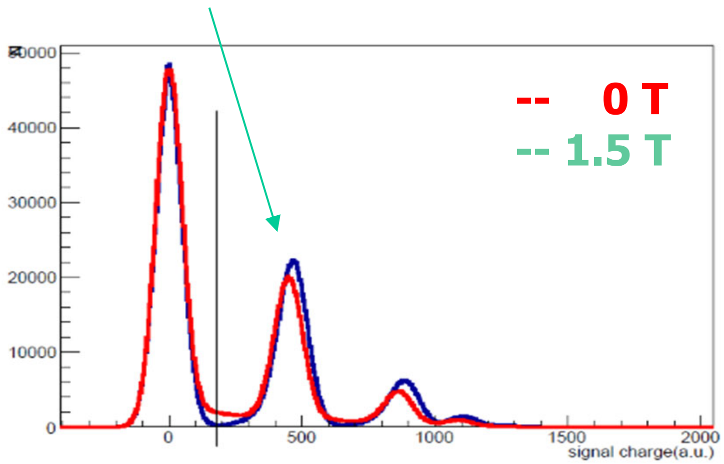

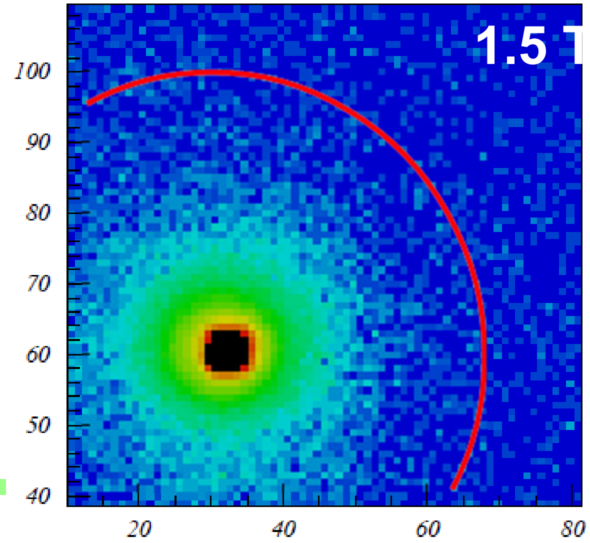

Solid state low light level photosensors: Silicon photomultipliers SiPM

An array of APDs operated in Geiger mode – above APD breakdown voltage (microcells or SPADs – single photon avalanche diodes)

Detection of photons:

- absorbed photon generates an electron-hole pair
- an avalanche is triggered by the carrier in the high field region → signal
- voltage drops below breakdown and avalanche is quenched (passive or active quenching)
- each triggered microcell contributes the same amount of charge to the signal

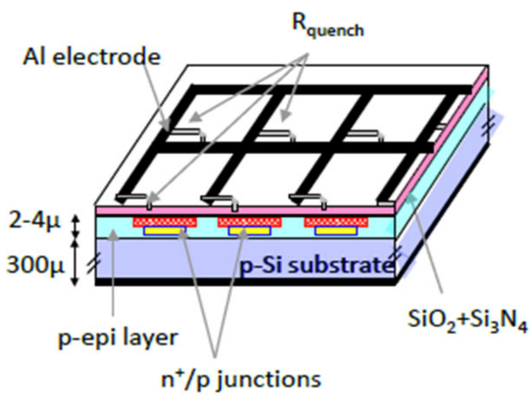

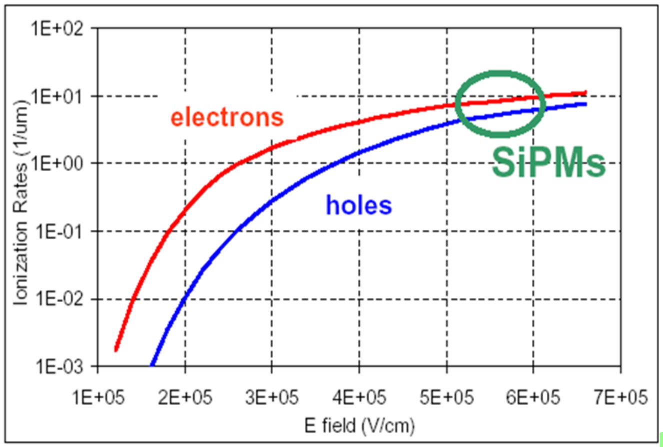

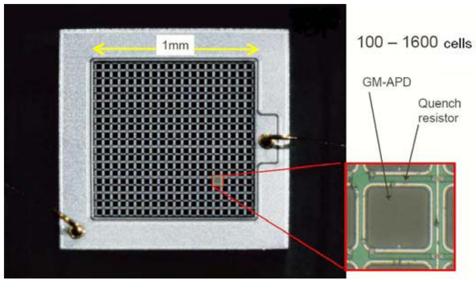

SiPM: noise

- Dark counts are produced by thermal generation of carriers, trap assisted tunnelling or band gap tunnelling
- Signal from dark counts is equal to the single photon response
- Typical rates went from $\approx 1\mathrm{MHz/mm^2}$ to below $100\mathrm{kHz/mm^2}$ for more recent devices
- Roughly halved for every -$8^o\mathrm{C}$
- Increases linearly with fluence

- Optical cross-talk produced when photons emitted in avalanche initiate signal in neighbouring cell, reduced by screening – trenches

- After-pulses produced by trap-release of carriers or delayed arrival of optically induced carrier in the same cell

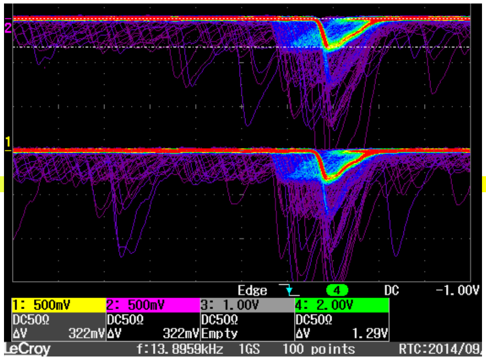

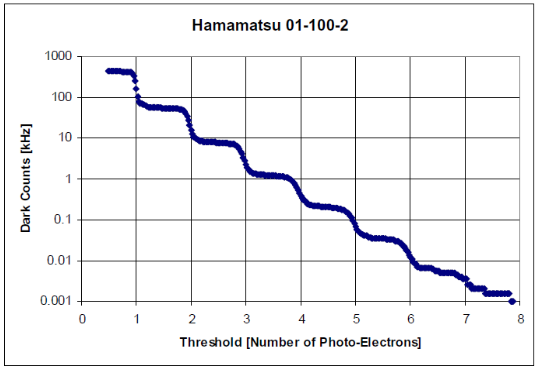

A. Gola et al. Sensors 19(2019)308

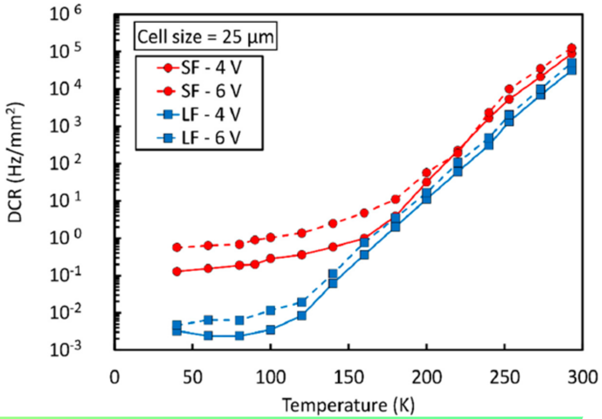

SiPM: parameter correlation

Higher overvoltage:

- ➢ higher field:
  - higher avalanche trigger probability → higher PDE
  - faster signal → better timing
- ➢ higher gain:
  - better signal to noise (electronic)
  - more optical cross-talk → higher ENF, worse timing
  - more after-pulses

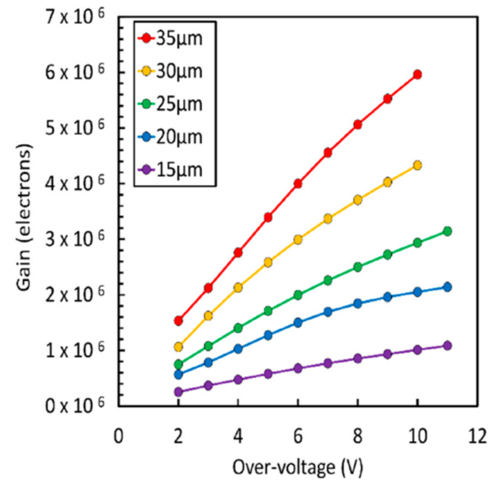

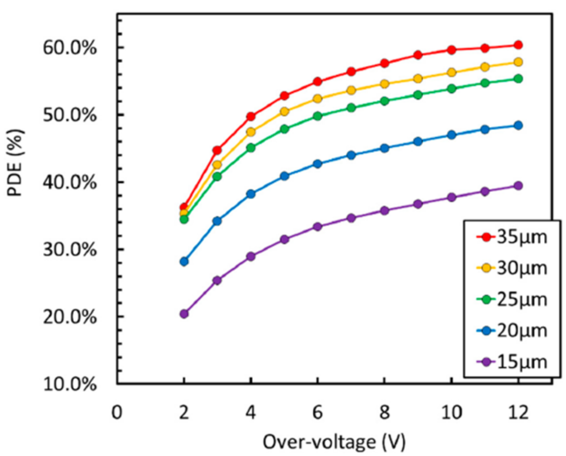

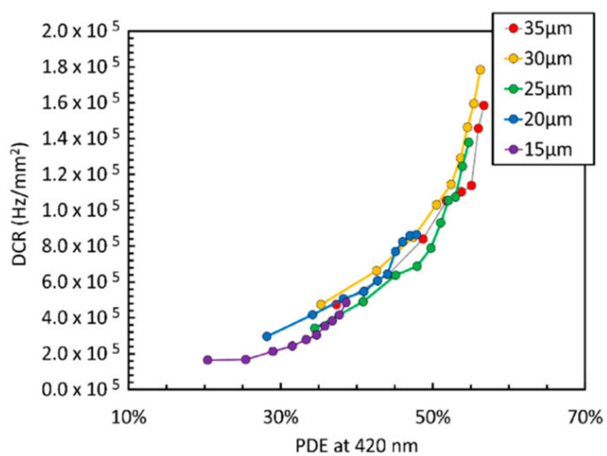

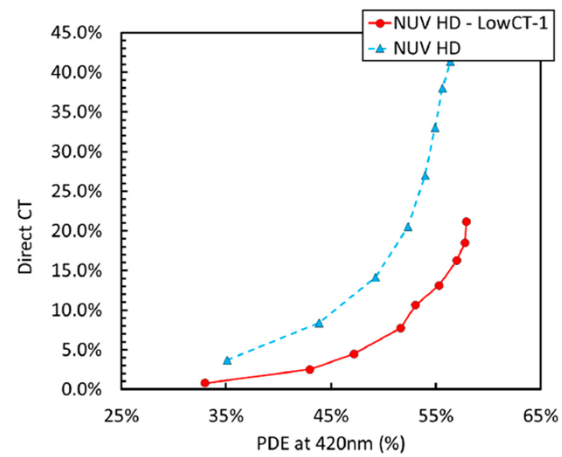

A. Gola et al. Sensors 19(2019)308

VUV SiPM for cryogenic applications

LAr, LXe applications:

- VUV sensitivity required:
  - 128 nm (LAr), 178 nm (LXe)
  - optimization of anti-reflective coating ARC
  - PDE $\approx 20\ \%$

- cryogenic temperatures:
  - low DCR $\approx 10\mathrm{mHz/mm^2}$ dominated by band-band tunnelling, reduced by low-field avalanche region
  - higher after-pulse rate $\approx 10\%$

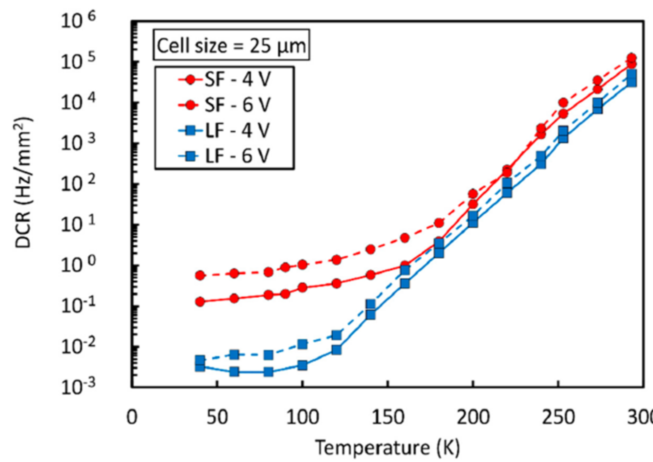

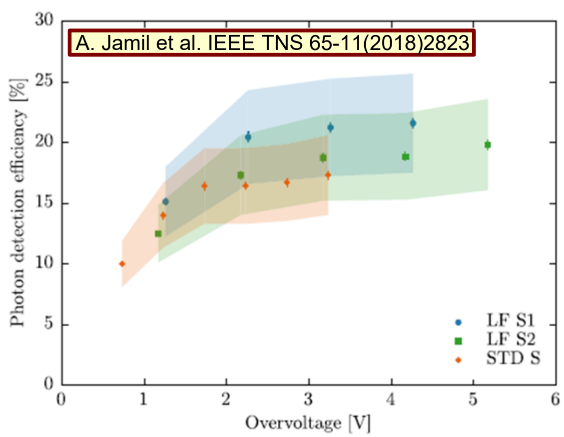

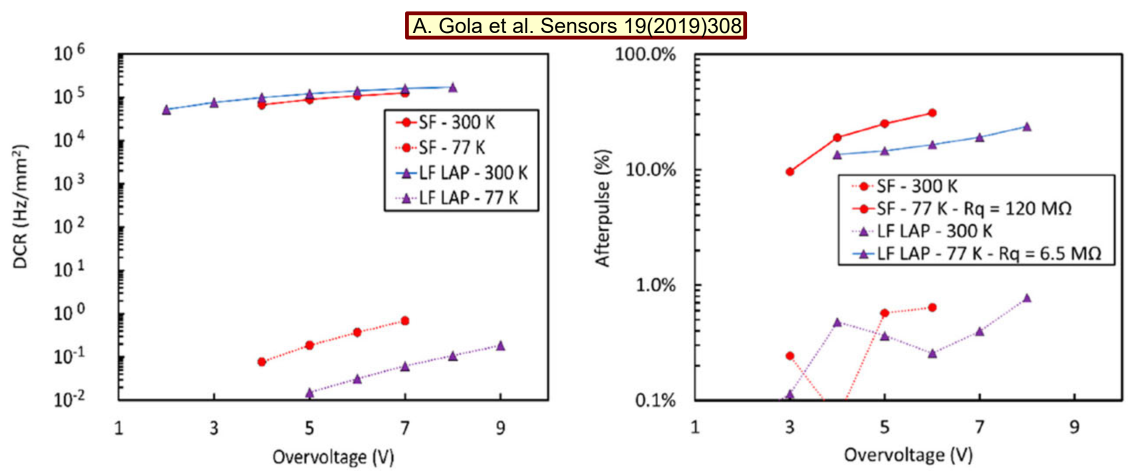

SiPM: single photon timing

Intrinsic TTS of SiPM microcells is extremely fast, $< 20\ \mathrm{ps}$ for single microcells (SPAD), but timing deteriorates for larger devices. The main contributions:

- nonuniformity within microcell (edges)
- spread between microcells
- overall SiPM capacitance
- λ dependence - tails

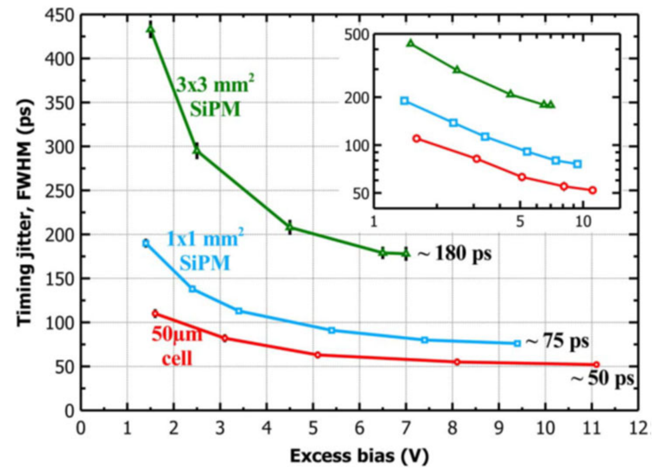

Comparison of timing properties for single $50\mu\mathrm{m}$ SPAD, $1 \times 1\ \mathrm{mm}^2$ and $3 \times 3\ \mathrm{mm}^2$ SiPMs with the same SPAD for microcells:

- timing improves with higher overvoltage – larger pulses, at the expense of increased SiPM noise
- best timing resolutions for single cell signals are $\sigma \approx 21\ \mathrm{ps}, 32\ \mathrm{ps}$ and $77\ \mathrm{ps}$
- TTS deterioration mainly due to a larger overall capacitance → reduced signal slope, $\sigma_t \approx \sigma_{el.} \left(\frac{dU}{dt}\right)^{-1}$

F. Acerbi et al. IEEE TNS 61(2014)2678

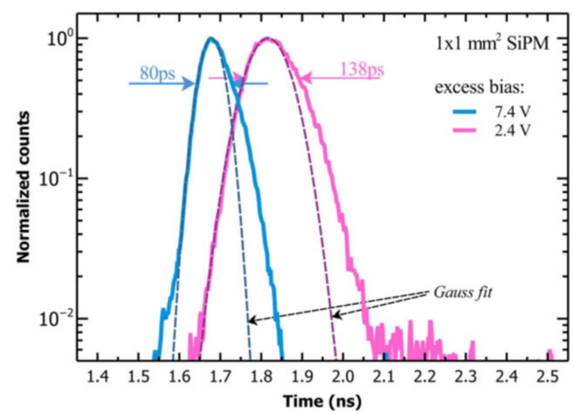

SiPM: timing variation

Variation of TTS over the device surface can contribute to overall time spread:

- variation within micro-cell
- variation for different micro-cells

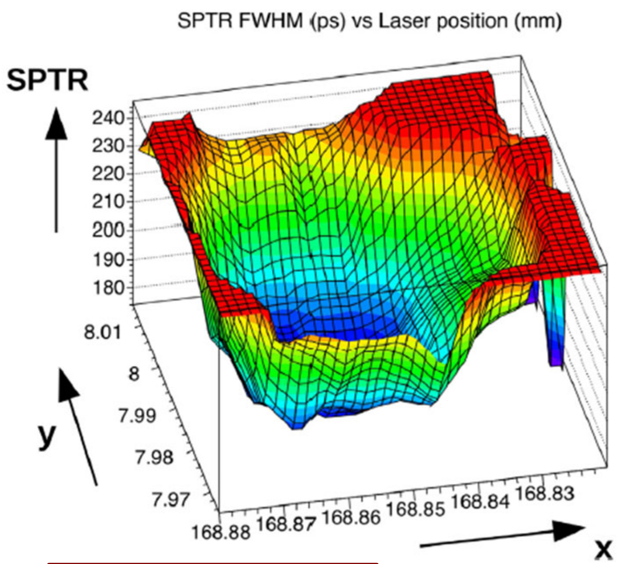

F. Acerbi et al. NIM A926(2019)16

KETEK PM3375TS-SBO (early design)

S. Korpar et al. @IEEE 2015

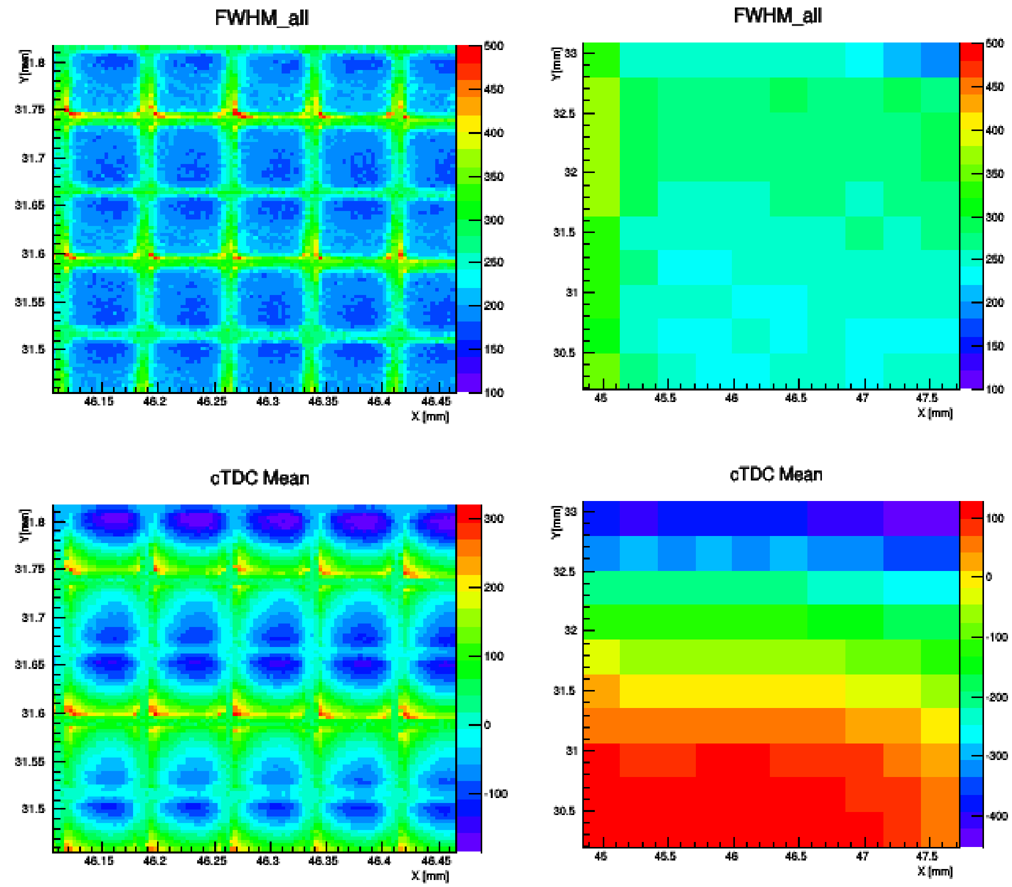

0.3 mm

2.5 mm

FBK: Masking of outer regions of micro-cells: Improve signal peaking and mask areas of micro-cell with worse timing

SiPM: timing for multi-cell signals

Optical cross-talk contribution to multi-cell signals spoils timing distribution – does not scale with $\frac{1}{N^{1/2}}$:

- two components for 2-micro-cell signals:
  - double photon events – proper scaling
  - single photon with cross-talk, timing somewhere between single and double micro-cell signals and resolution is worse
- ratio between contributions changes with light intensity confirming optical cross-talk origin
- even more components for multi-micro-cell signals

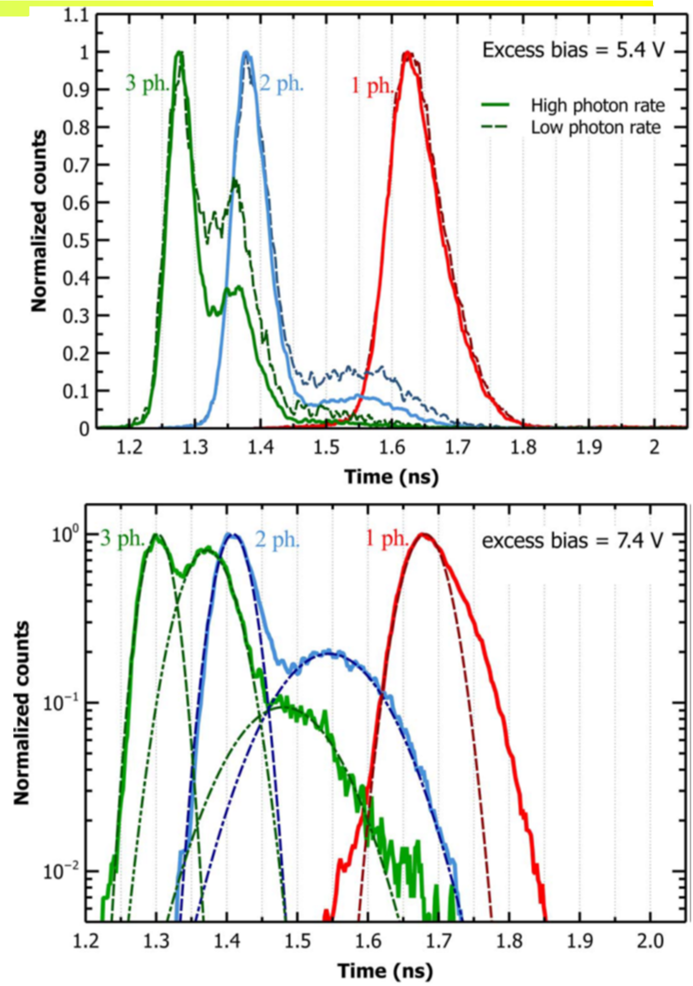

F. Acerbi et al. IEEE TNS 61(2014)2678

SiPM: timing test with pico-second laser

- AdvanSiD SiPM ASD-NUV3S-P-40
- OV=6V, T=-25$^{o\,C}$
- blue laser λ =408nm, ~ 35ps FWHM

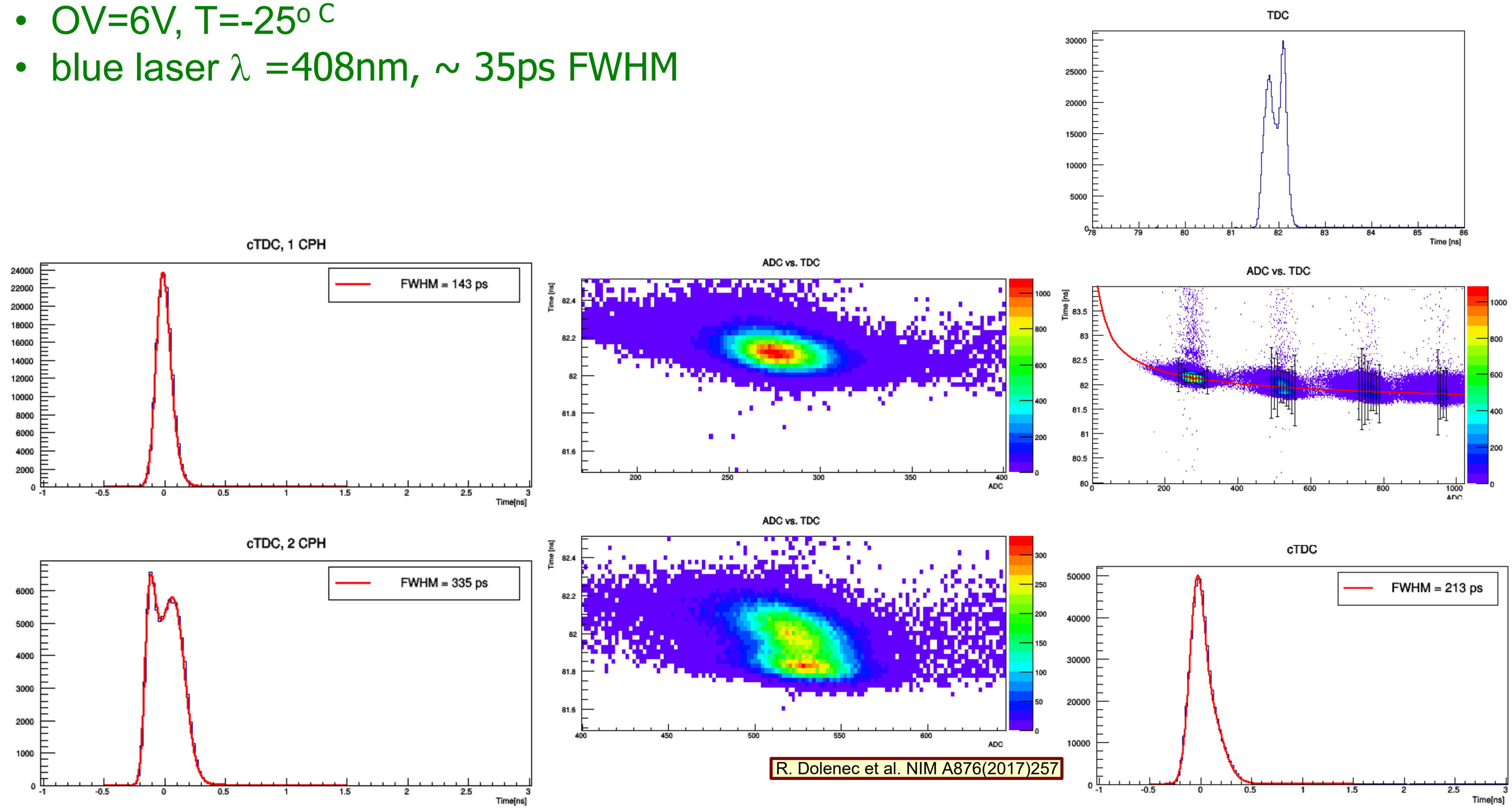

Reduction of optical crosstalk

Starting from the NUV-HD technology, FBK and Broadcom jointly developed the NUV-HD-MT technology, adding metal-filled deep trench isolation to strongly suppress optical crosstalk.

Other changes: low electric field variant, layout optimized for timing.

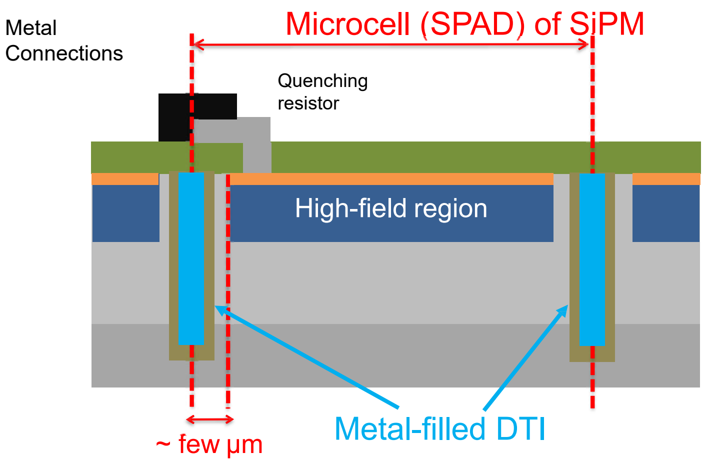

Conceptual drawing of the NUV-HD-MT, with the addition of metal-filled Deep Trench Isolation.

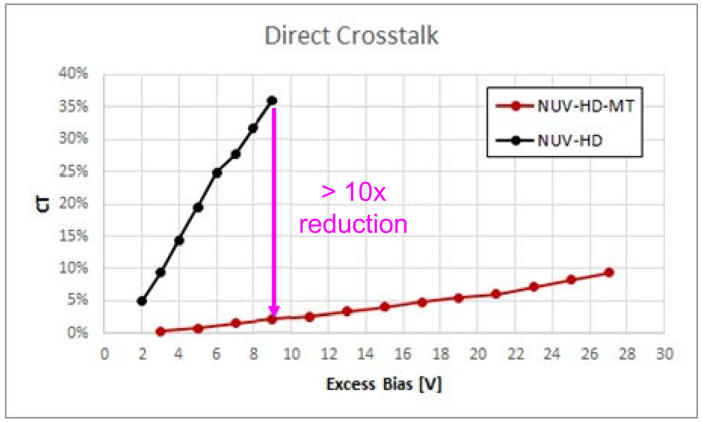

Reduction of optical crosstalk probability in NUV-HD-MT, compared to the "standard" NUV-HD. Measurement without encapsulation resin, i.e. only considering internal crosstalk probability.

A. Gola, RICH2022

Light concentrators

At the device level (lenses, Winston cones):
• reduce active are – reduce DCR (tolerate higher fluences)
• use smaller faster devices
At the micro-cell level (micro-lenses, diffractive lenses, meta lenses):
• compensate for low fill factor – small cells, dSiPM
• concentrate light in cell centre – better timing

Higher concentration – narrower angular acceptance

Imaging light concentrators:
• smaller photon impact angles on the sensor
• can be used with position sensitive arrays

Non-imaging light concentrators:
• larger photon impact angles on the sensor – directly coupled to sensor

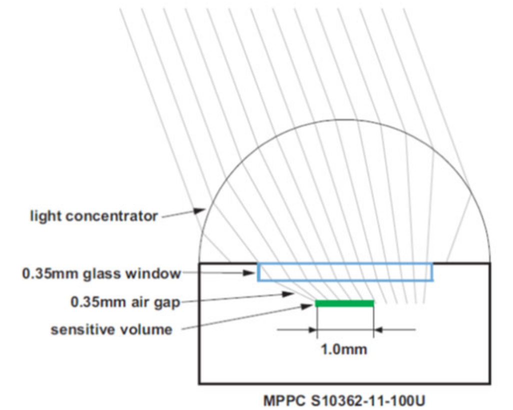

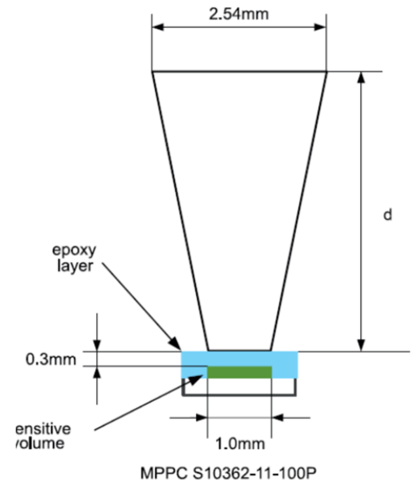

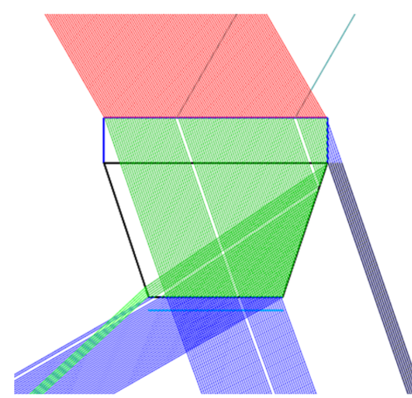

SiPM RICH with light concentrators

RICH photon detector module prototype:

- Hamamatsu 64 channel MPPC module S11834-3388DF, 8×8 array of $3 \times 3\ \mathrm{mm}^2$ SiPMs @ $5\ \mathrm{mm}$ pitch
- matching array of quartz light concentrators used
- two $20\ \mathrm{mm}$ thick aerogel tiles in focusing configuration ($\mathrm{n} = 1.045, 1.055$)
- tested in $5\ \mathrm{GeV}$ electron beam at DESY

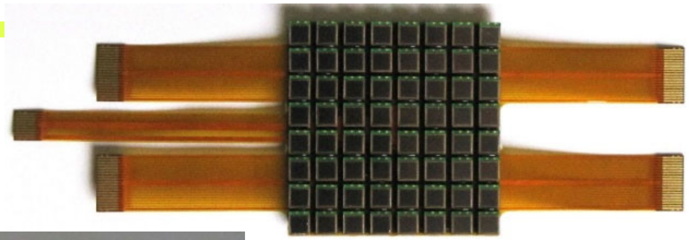

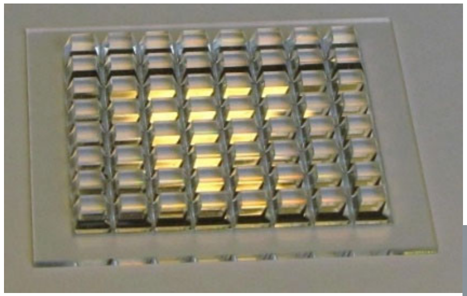

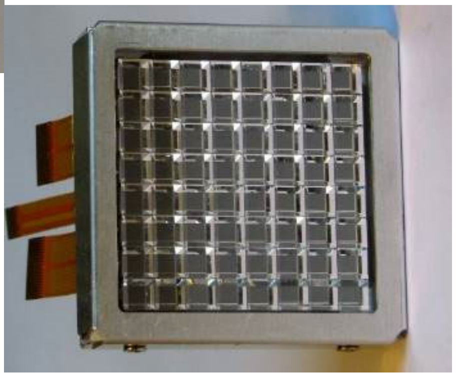

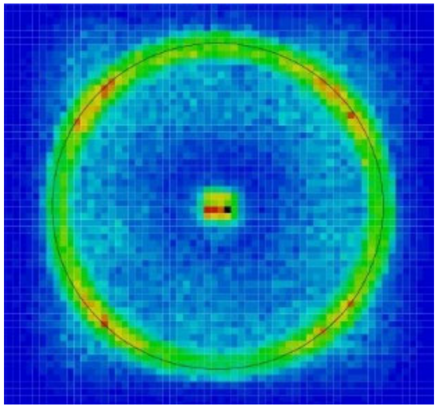

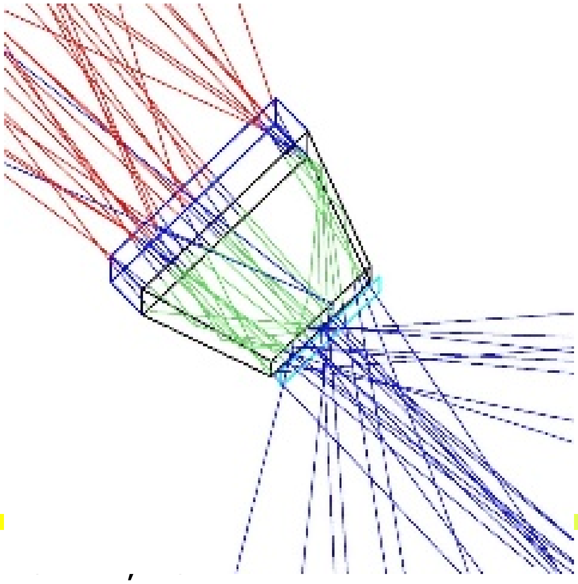

E. Tahirović et al., NIM A787 (2015) 203

Microlenses

Micro-lens array coupled to SPAD array

- CMOS SPAD array, 128x128 $6\mu m$ diameter @$25\ \mu m$ pitch – 5% fill factor
- matching polymer plano-convex micro-lens array

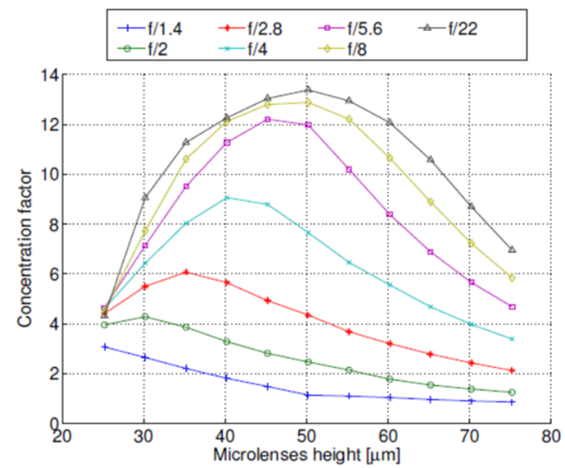

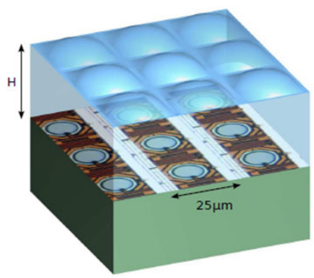

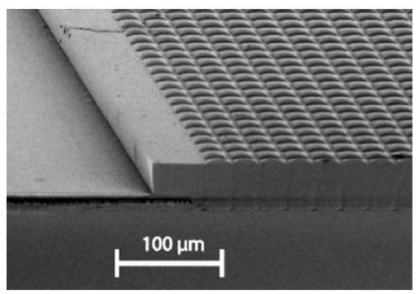

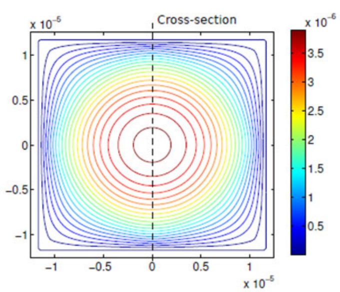

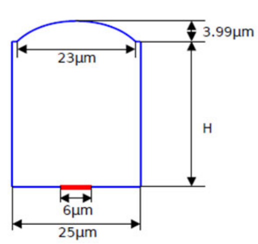

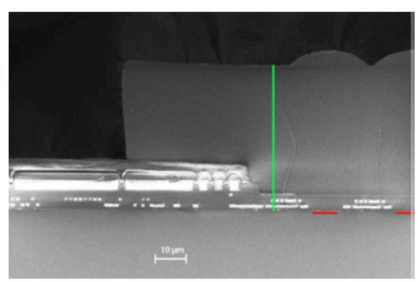

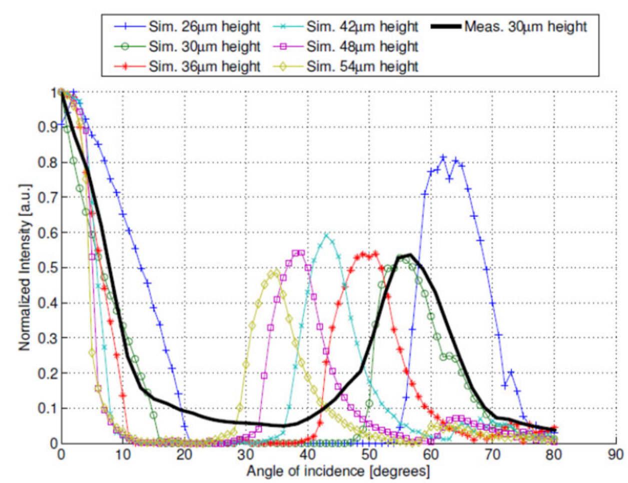

J.M. Pavia et al. Opt.Exp. 22-4(2014)4202

SiPMs: Radiation damage

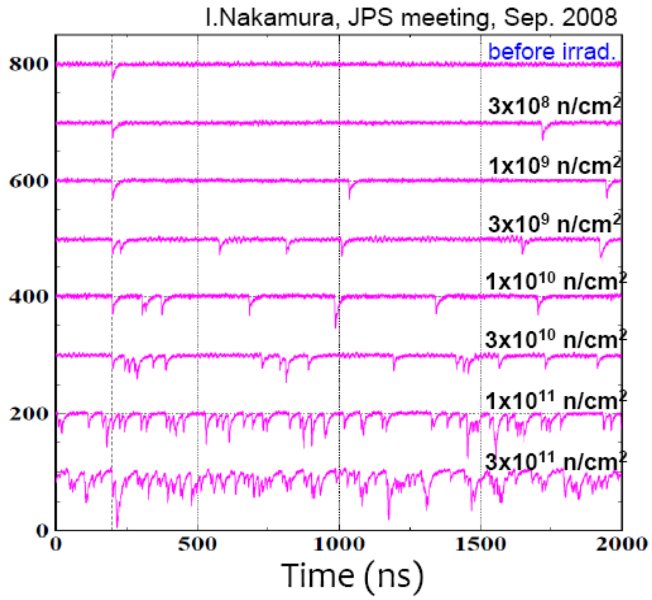

Show stopper at fluences above $\sim 10^{11}$ in case single (or few) photon sensitivity is required!

(e.g. expected fluence in the ARICH area of Belle II: 2-20 10^{11} n cm^{-2})

→ Use of wave-form sampling readout electronics

→ Operating the SiPMs at lower temperature

→ Annealing periodically (annealing at elevated temperature is preferred)

→ Reducing recovery time to lower cell occupancy

→ Radiation resistant SiPMs, other materials?

SiPMs: Radiation damage

A. Gola, RICH2022

Beyond $10^7 \div 10^8$ n_{eq}/cm^2 little correlation between the DCR before and after irradiation:

- All technologies seem to “converge” towards similar values
- Independence of bulk damage from contaminants in the SiPM starting material?

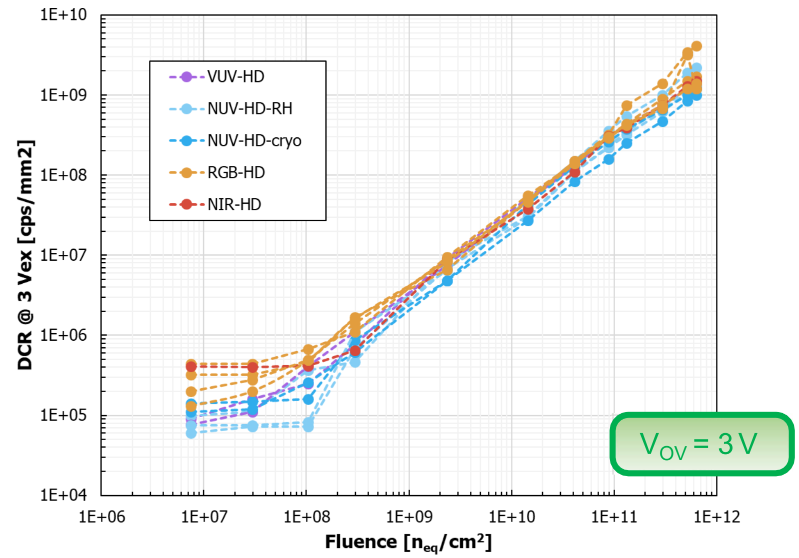

DCR (dark count rate) vs fluence

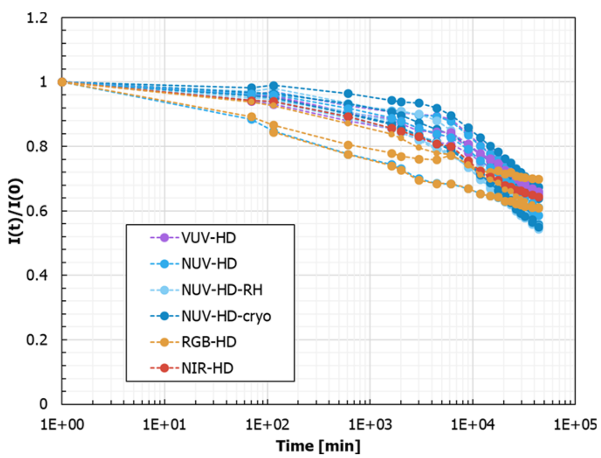

Room temperature annealing (20-25°C) for samples irradiated to $6.4 \cdot 10^{11}$ 1 MeV n_{eq}/cm^2

Little effect, knee point at around $1.5 \cdot 10^3$ min (~1 day)

A. Gola, RICH2022

SiPMs: Radiation damage, annealing at elevated temperatures

Dark counts at -30C of a Hamamatsu S13360-1350CS SiPMs: non irradiated (blue) and irradiated up to 10^{11} (yellow), 10^{12} (green) and 10^{13} (orange) n_{eq}/cm^2

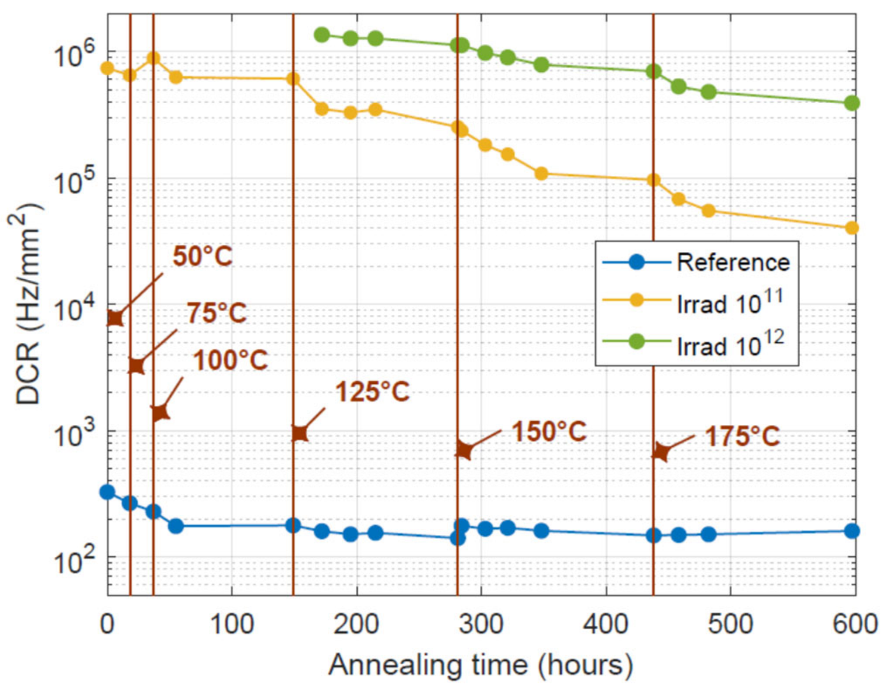

M. Calvi et al., NIMA 922 (2019) 243-249

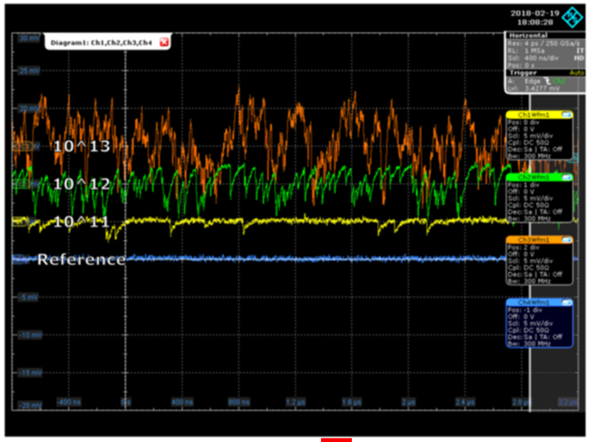

annealing

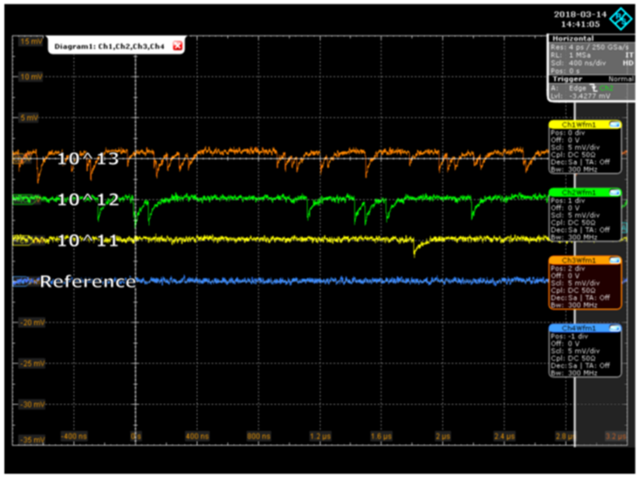

SiPMs: annealing after irradiation

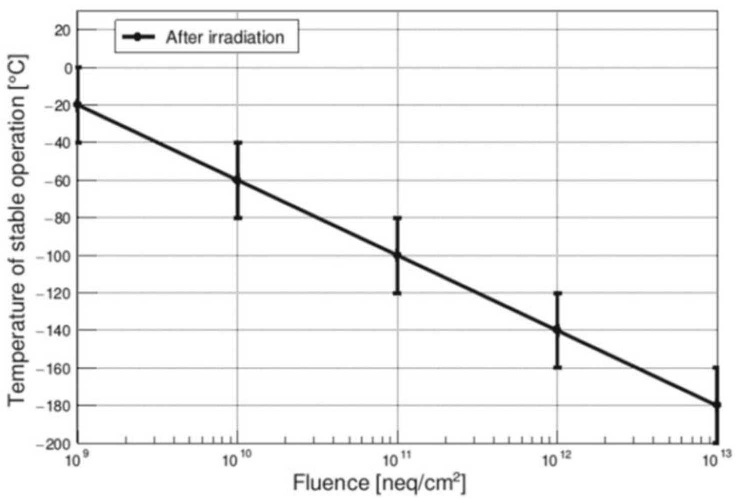

The temperatures at which single photon can be resolved at an overvoltage of 9 V vs. different irradiation levels. The error bars indicate the 40◦C steps in which the measurements were carried out.

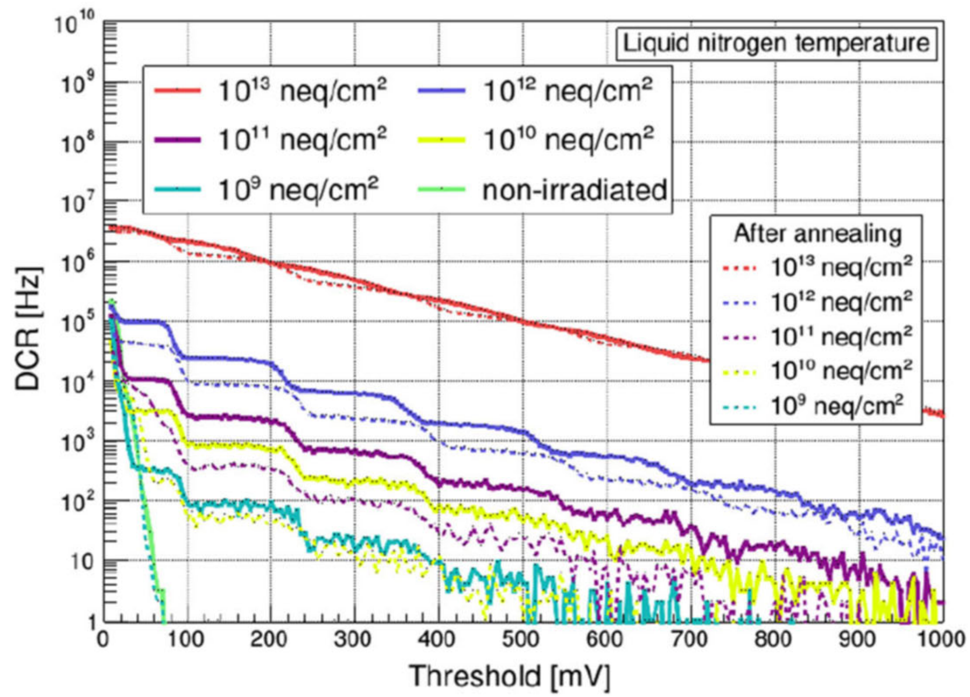

DCR measurements for each of the SiPMs at liquid nitrogen temperature before and after the annealing (dashed)

Studies for Belle II ARICH upgrade

Dania Consuegra Rodríguez et al, Eur. Phys. J. C (2024) 84:970

Belle II detector: subsystems with R&D for potential photosensor upgrades

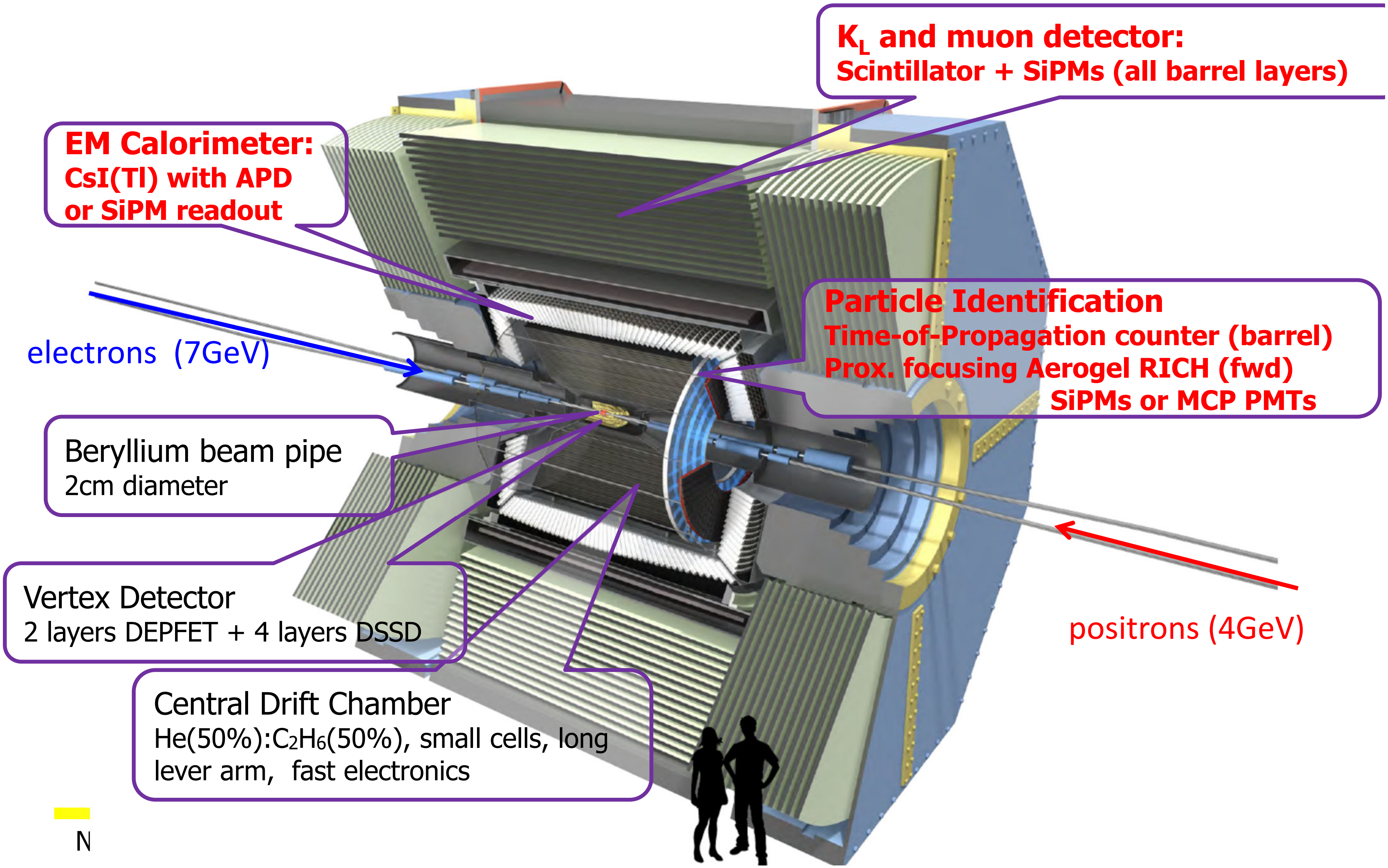

N

Possible Upgrade of ARICH

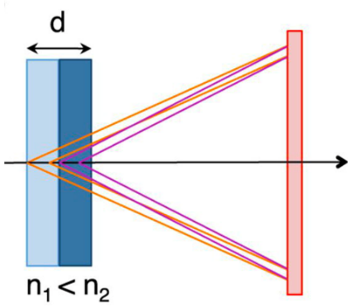

- double layer focusing aerogel radiator (20+20 mm)
- 160 mm expansion gap
- photon detector : 420 HAPDs - Hybrid Avalanche Photo Detectors

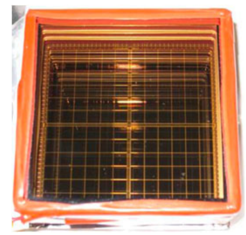

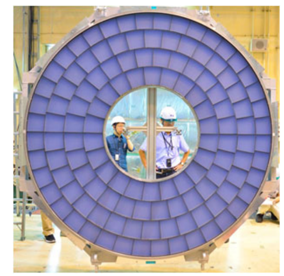

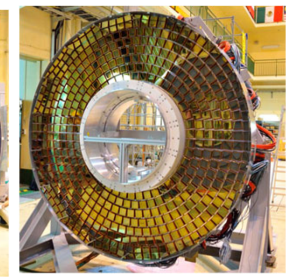

ARICH K efficiency vs. π misidentification probability

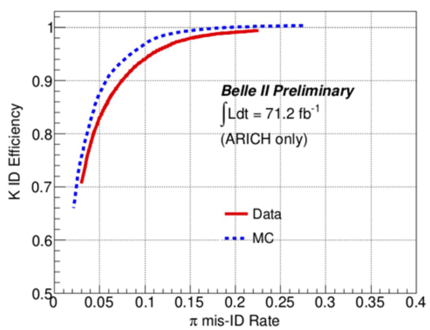

Belle II ~2033

In case of a further increase of the luminosity beyond the design value

- Higher backgrounds
- HAPD – accumulated dose too high - will not be able to operate
- Search for new technologies:
  Candidates: SiPM, MCP-PMT

LAPPDs?

Possible LAPPD tiling scheme

$20x20cm^2$
$10x10cm^2$

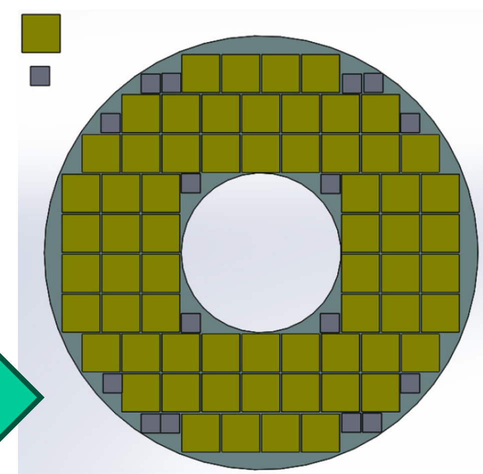

LAPPD evaluation

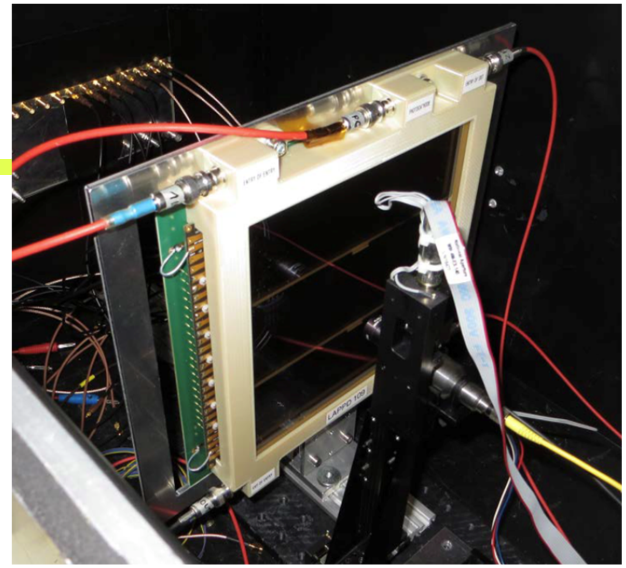

- Two 10 um devices acquired
- LAPPD installed in the dark box:
- CAEN HiVolta (DT1415ET), 8 Ch Reversible 1 kV/1 mA Desktop HV Power Supply – floating channels
  - 1 kV/1 mA and 0.6 W(!) per channel
- Measure response in the lab with modular electronics, FastIC and PETSys
- Standard setup with QDC, TDC, 3D stage ...
  - TDC value corrected for time-walk
- ALPHALAS PICOPOWER™-LD Series of Picosecond Diode Lasers –405 nm
  - FWHM ≈20ps
  - light spot diameter on the order of 100μm
- Custom segmentation to study the capacitive coupling and the charge spread

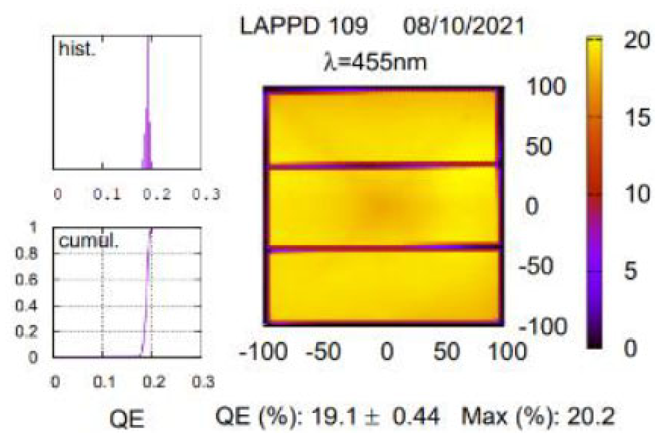

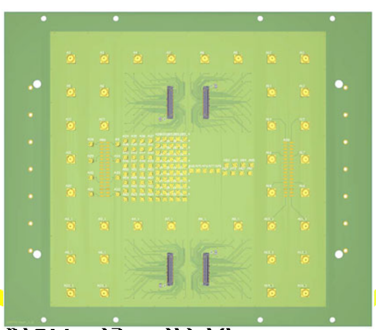

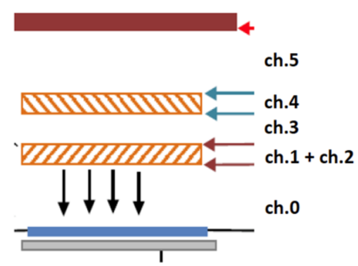

LAPPD #162 timing and signal charge

- oscilloscope screenshot with laser spot at the center of D2 pad
- TDC(yellow) and pulse integral(blue) histograms
- TDC main peak FWHM is 67 ps corresponding to sigma below 30 ps.
- Average pulse integral is 25 pVs -> ~ 3e6 electrons

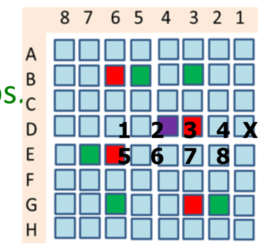

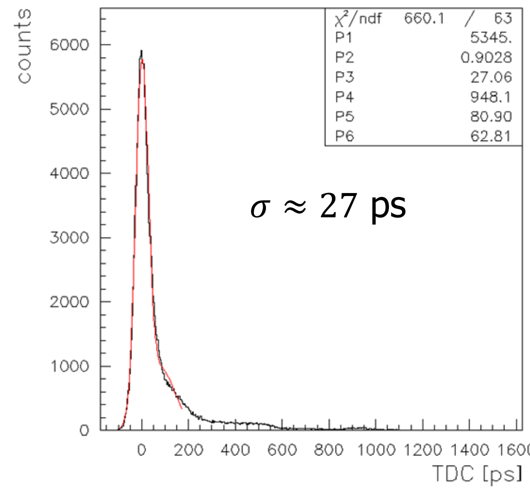

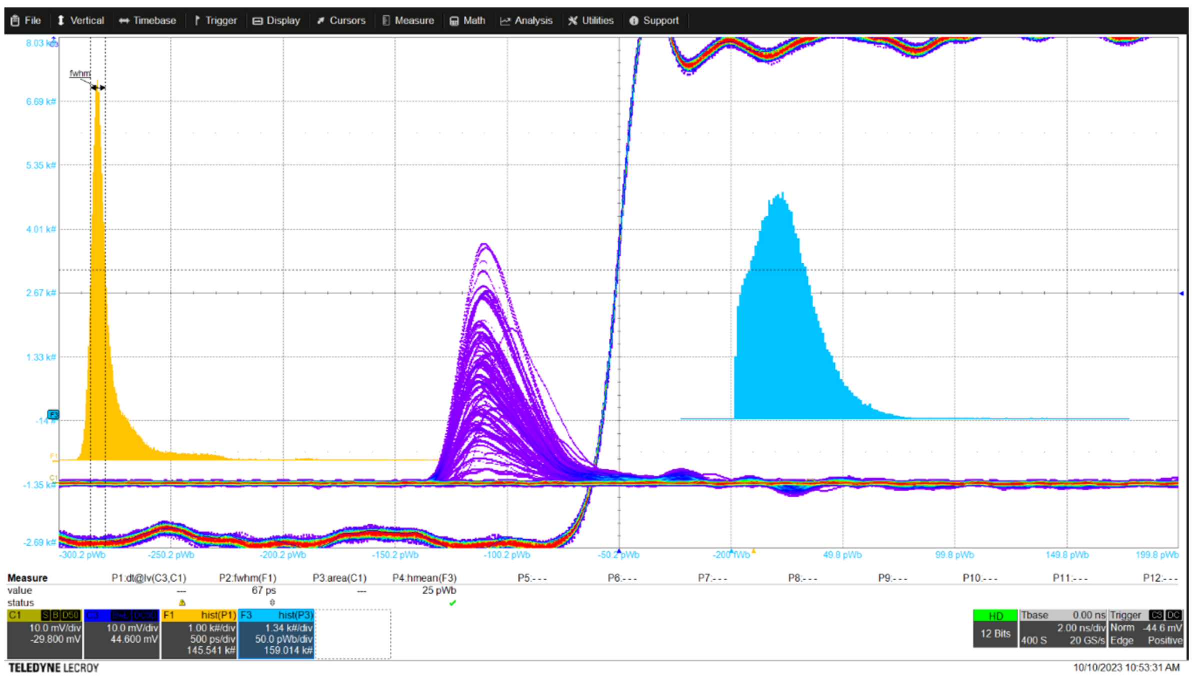

- applied voltages and currents
- Anode-MCP2out, ... , MCP1in-PC (units V,uA)

VSet	VMon	IMon	ISet
200.00	200.18	0.3500	5.00
825.00	825.62	176.7500	200.00
200.00	200.22	0.0690	5.00
825.00	825.52	154.2340	200.00
200.00	199.98	0.0930	5.00

R.Pestotnik, ARICH meeting@ 47th B2GM Jan 26 2024 44

LAPPD – charge sharing in Gen II capacitively coupled electrode readout

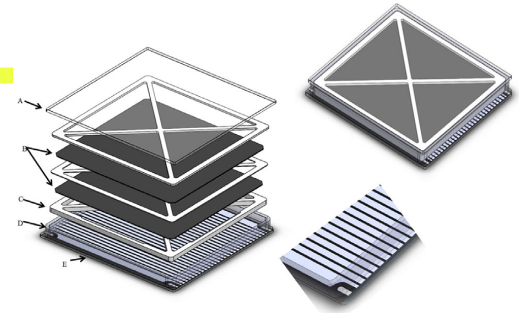

- fraction of the signal on channel 3 vs laser spot x position: $f(x) = \frac{q_3}{\sum_i q_i}$
- scan between the centres of pads 2 and 3 (top)

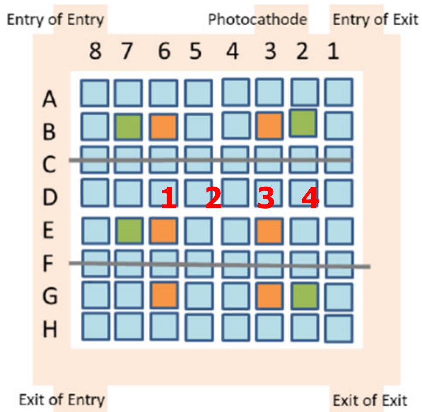

- central slice where signal is equally split between the pads (bottom)
- narrow peak is due to the light spot size and photoelectron spread
- longer tail from photoelectron backscattering - $\approx$ 6 mm on each side $\rightarrow \approx$ 3 mm PC – MCP1 distance

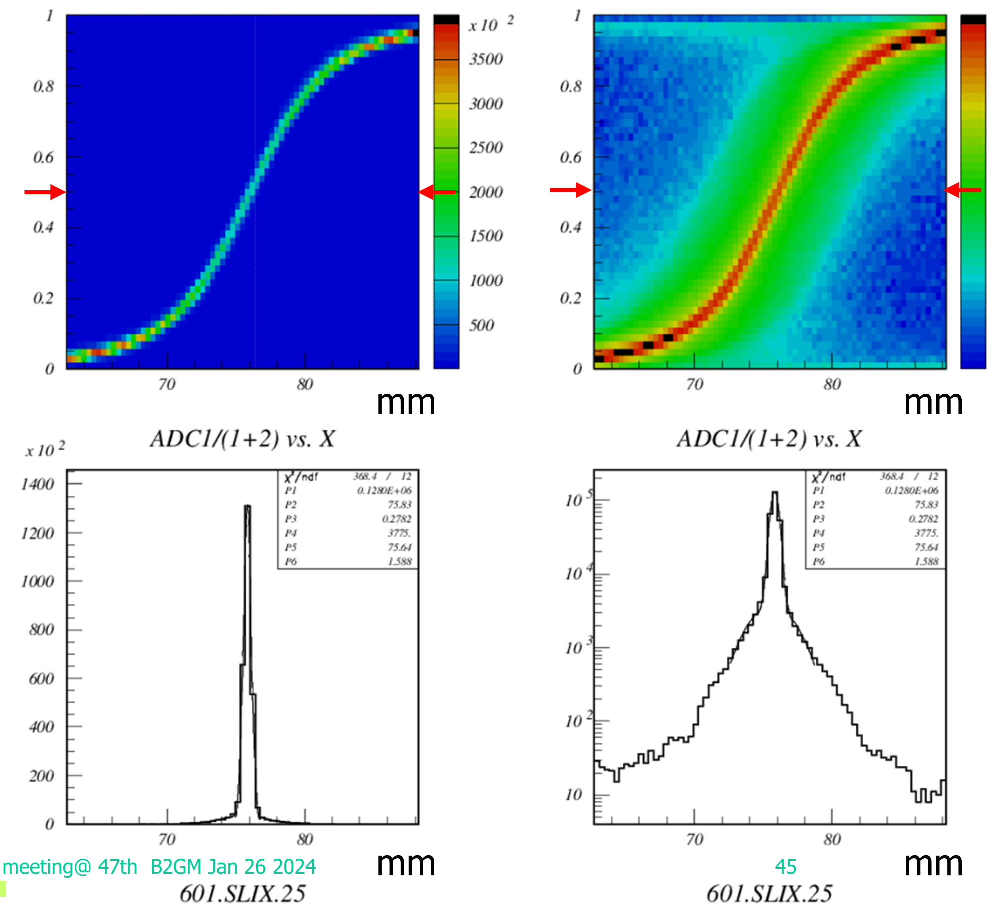

R.Pestotnik, ARICH meeting@ 47th B2GM Jan 26 2024

Charge sharing for 2 samples

#162 (2mm ceramic) vs.
#109 (5mm borosilicate window)

- An example plot for charge sharing between pads D3-D5 for:
  - 162 (top) compared with similar plot for
  - 109 (bottom).
- One can see reduced signal spread as expected.
- From backscatter component range (~2mm) one can also see that PC-MCP1 in distance was reduced:
  - from about 3mm (109)
  - to about 1mm (162).

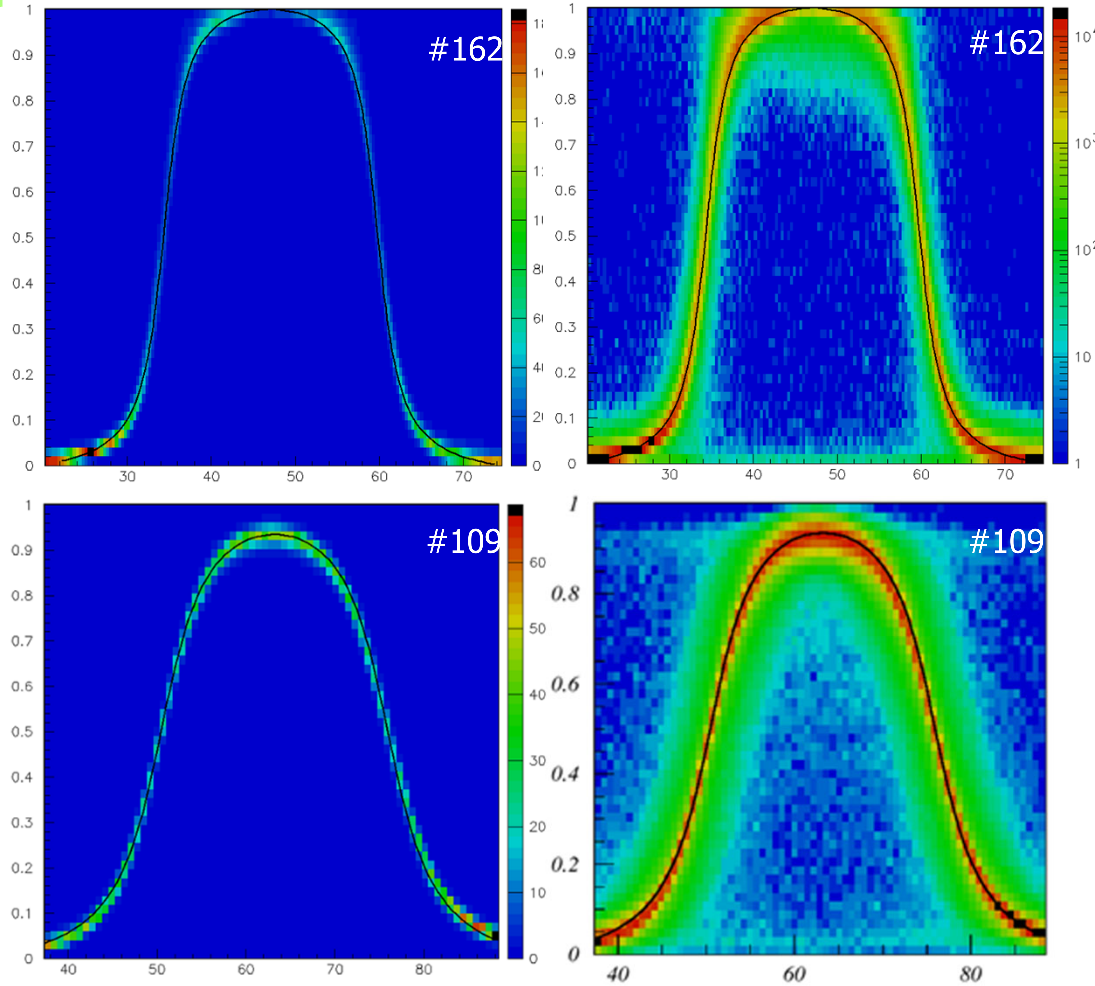

R.Pestotnik, ARICH meeting@ 47th B2GM Jan 26 2024 46

LAPPD – timing distribution

- measured timing distribution typical for MCP-PMT
- main prompt peak with some inelastic and elastic backscattering contribution
- additional small peak at about 1 ns delay probably due to some reflection (light?), delay not affected by PC-MCP1 voltage
- The plot is for the PC-MCP1 voltage of 150 V and recommended HV for others

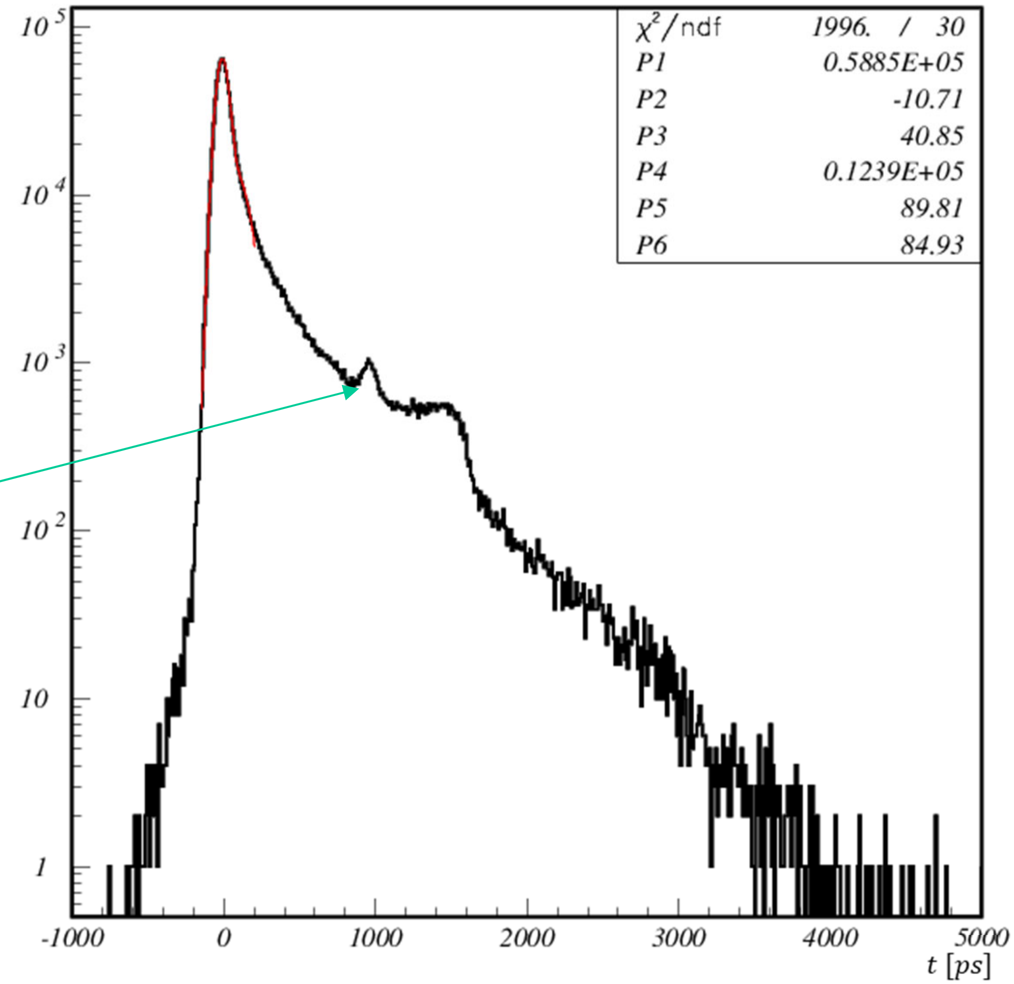

S. Korpar et al., to be submitted to NIMA

LAPPD – timing vs PC-MCP1 voltage

Time-walk corrected TDCs for different PC-MCP1 voltages

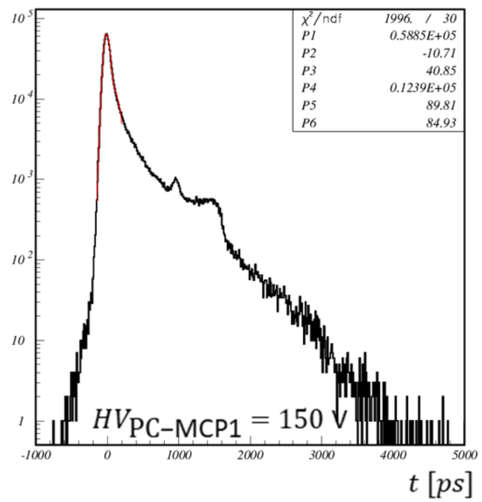

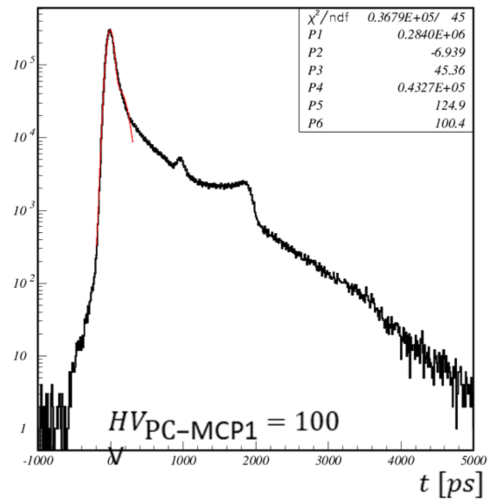

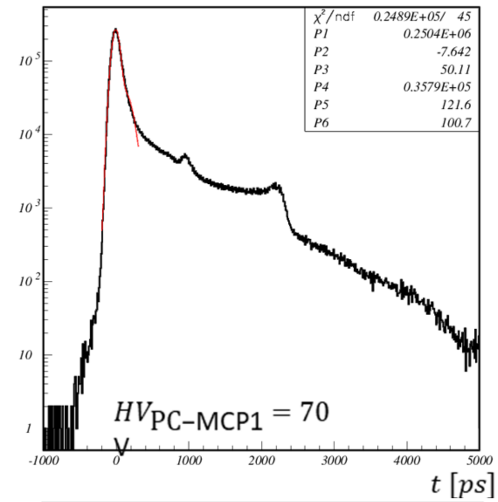

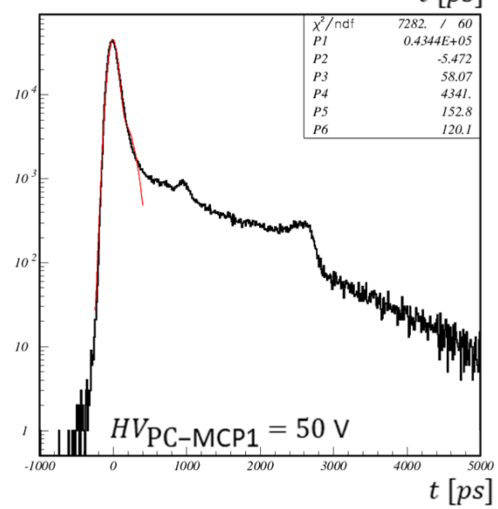

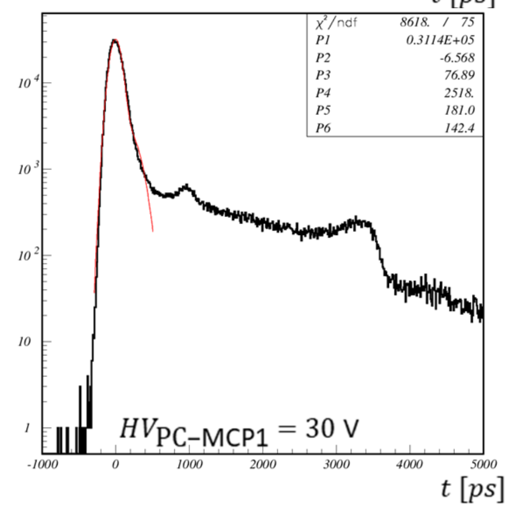

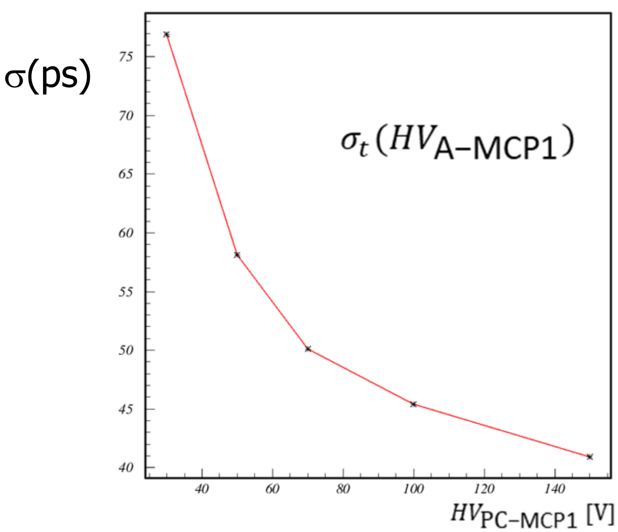

Time resolution vs PC-MCP1 voltage

KLM upgrade, option 1

Regular scintillator strips, original design

Scintillator with a reflective layer

WLS fiber

SiPM

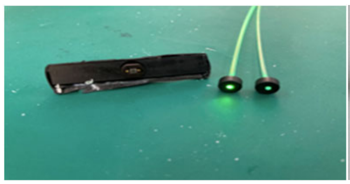

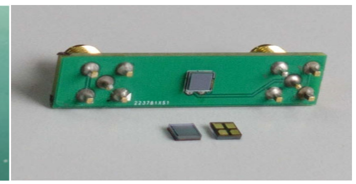

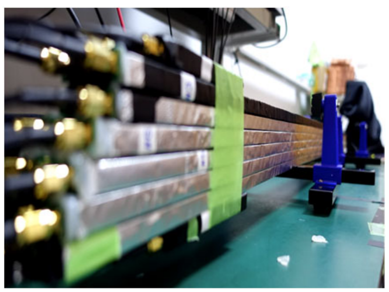

1.5 m scintillation detector

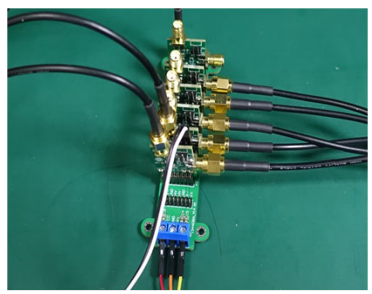

Preamplifier

Performance in cosmic ray testing

H.Y. Zhang et al.,
arXiv:2312.02552
Accepted by JINST

Single channel:

$\epsilon > 95\%$

$\sigma_T < 1.5\ ns$

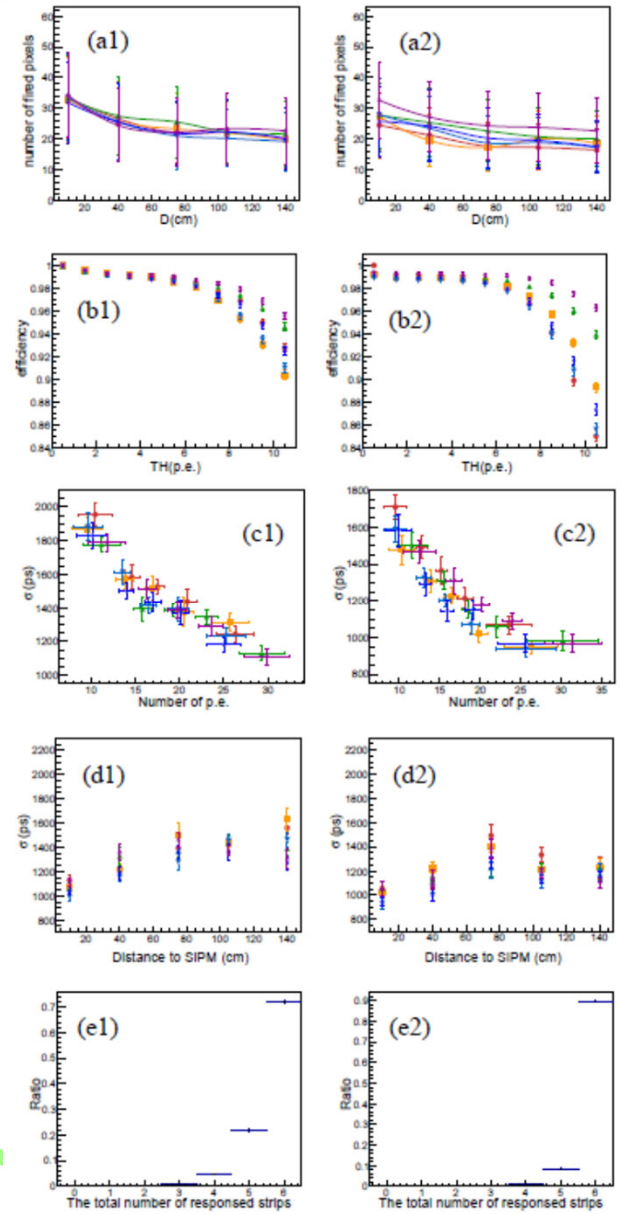

KLM upgrade, option 2

Precise time measurement – for example for the time-of-flight measurement of K_L velocity/momentum

Solid scintillator (no WLS fiber)

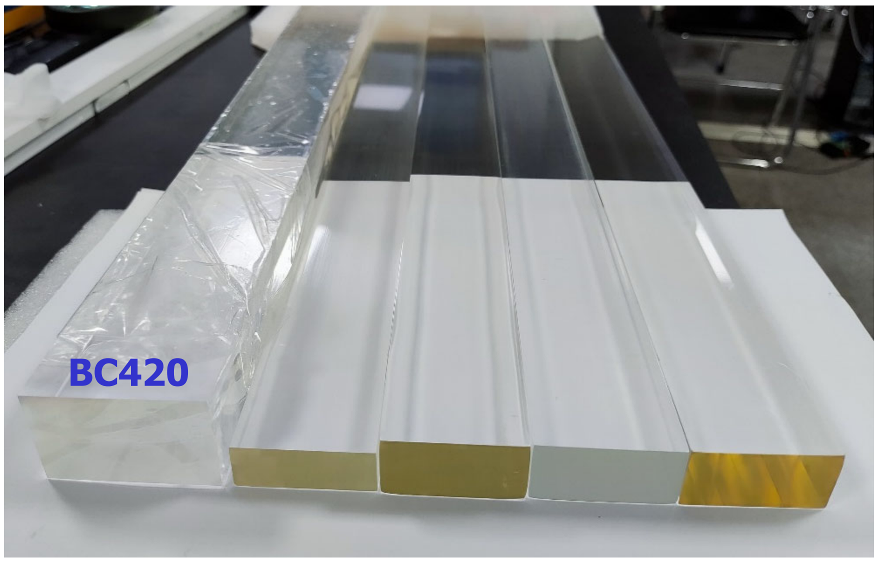

SAINT-GOBAIN

高能科迪 GAONENGKEDI

Multiple SiPMs

HAMAMATSU PHOTON IS OUR BUSINESS

NDL

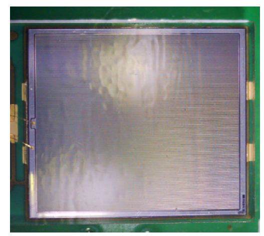

S13360-6025PE

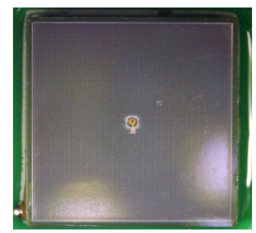

S14160-6050HS

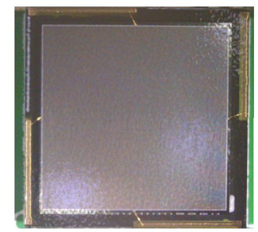

EQR1511-6060D-S

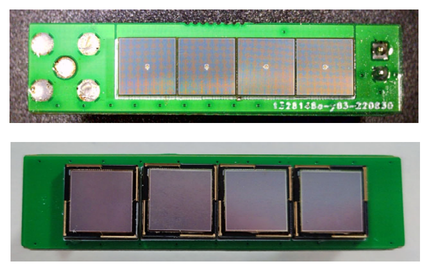

4×SiPM

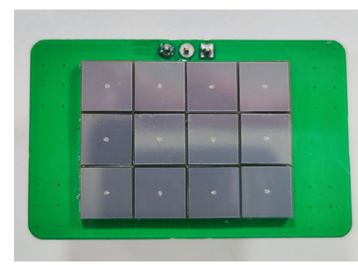

12×SiPM

- ➢ Thicker scintillators with longer attenuation lengths and large areas of SiPM can improve photon collection – and time-of-arrival resolution.

KLM upgrade, option 2, test results

Time resolution of a long scintillator bar (GNKD_new, 2cm)

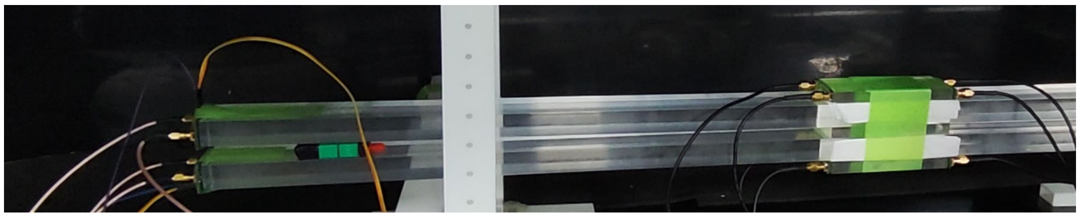

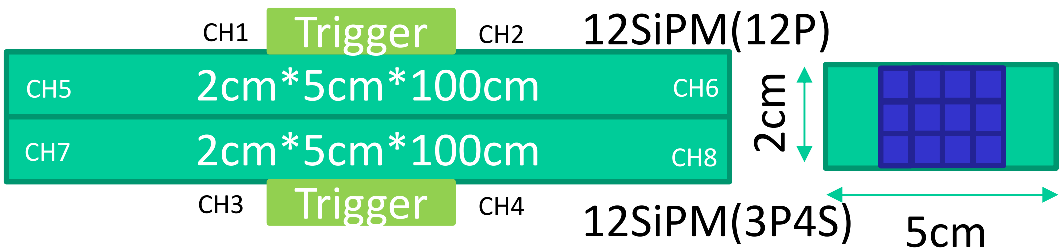

Timing with a custom-developed fast amplifier

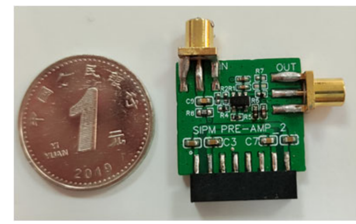

X.Y. Wang et al.,
Nucl. Scin. Tech. 34, 169 (2023)

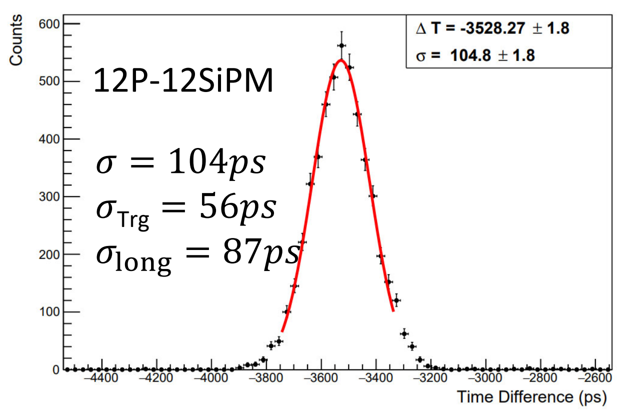

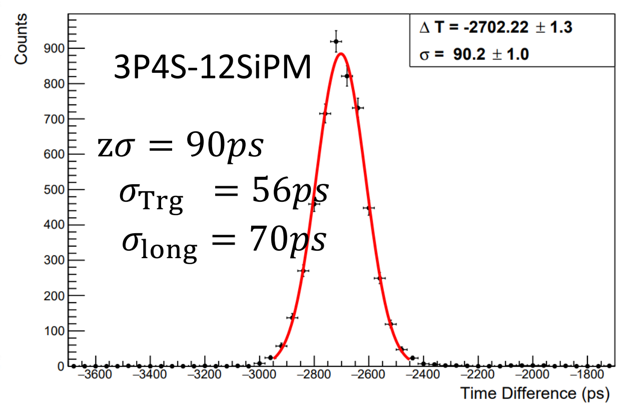

Summary and outlook

Next generation of experiments in particle physics: faster timing, wider spectral range and improved radiation tolerance.

Many new interesting developments are underway, in particular in SiPMs and MCP-PMTs – not all of them could be covered in this talk.

A detector R&D collaboration (DRD4) has been set-up to facilitate collaboration in this area of research, started in January 2024. Worth considering to join one of the activities.

At Belle II, we are investigating possible upgrade scenarios, and carrying out very interesting photosensor R&D.

Back-up slides

More to read

The write-up of a talk at PSD13 (Oxford, 2023) that covers most of the topic discussed here (P.K., NIMA 1065 (2024) 169482) is available (open access) at https://doi.org/10.1016/j.nima.2024.169482

Web pages of our detector lab https://photodetectors.ijs.si
and analysis activities https://faime.ijs.si/

DRD4 Collaboration https://drd4.web.cern.ch/

MCP PMT readout: capacitive coupling vs. internal anodes

Secondary electrons spread out when traveling from the MCP-out electrode to the anode and can hit more than one anode → Charge sharing

Can be used to improve spatial resolution.

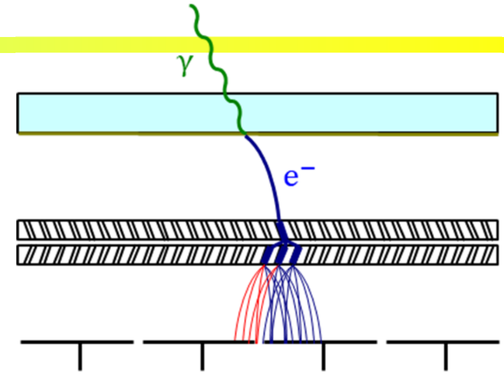

LAPPD (capacitive coupling through the backplane)

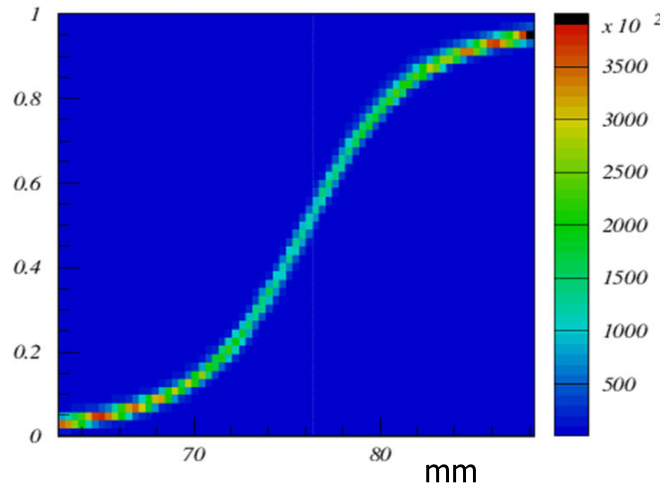

BURLE/Photonis PLANACON (internal anodes)

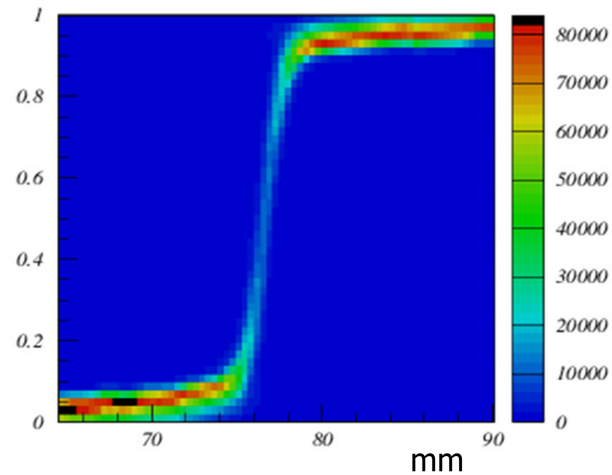

Fraction of the charge detected by the right pad as a function of red laser spot position

Capacitive coupling vs. internal anodes: signal spread comparison for two MCP PMTs with the same pad size, same range: charge sharing is more effective for capacitive coupling (spreads over larger area) - advantage or not: depends on the usage